

Evaluating Chemical Ligation Techniques for the Synthesis of Block Copolypeptides, Polypeptoids and Block Copolypept(o)ides: A Comparative Study

K. Klinker, R. Holm, P. Heller, M. Barz

Institute of Organic Chemistry, Johannes Gutenberg-Universität Mainz, Duesbergweg 10-14, 55128 Mainz, Germany

Supporting Information

1. NMR Data

1.1 NCAs

1.1.1 SarNCA

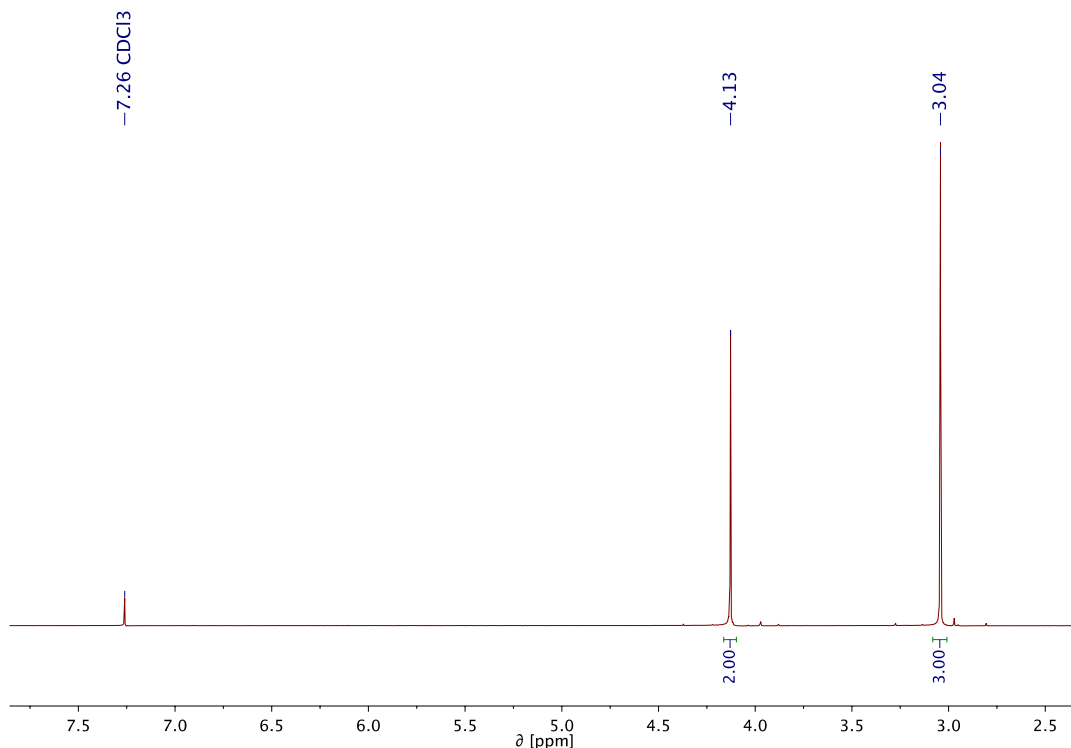


Figure 1: ¹H NMR spectrum of SarNCA in CDCl_3 (300 MHz).

1.1.2 Glu(OBzl)NCA

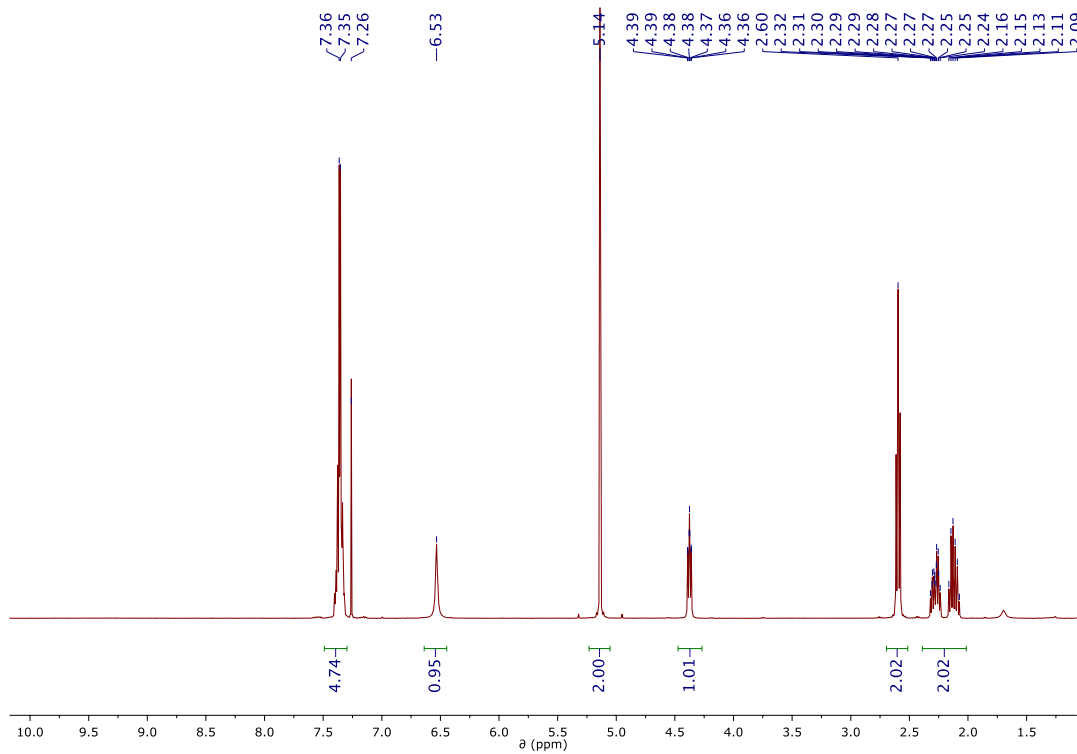


Figure 2: ^1H NMR spectrum of Glu(OBzI)NCA in CDCl_3 (300 MHz).

1.1.3 Lys(TFA)NCA

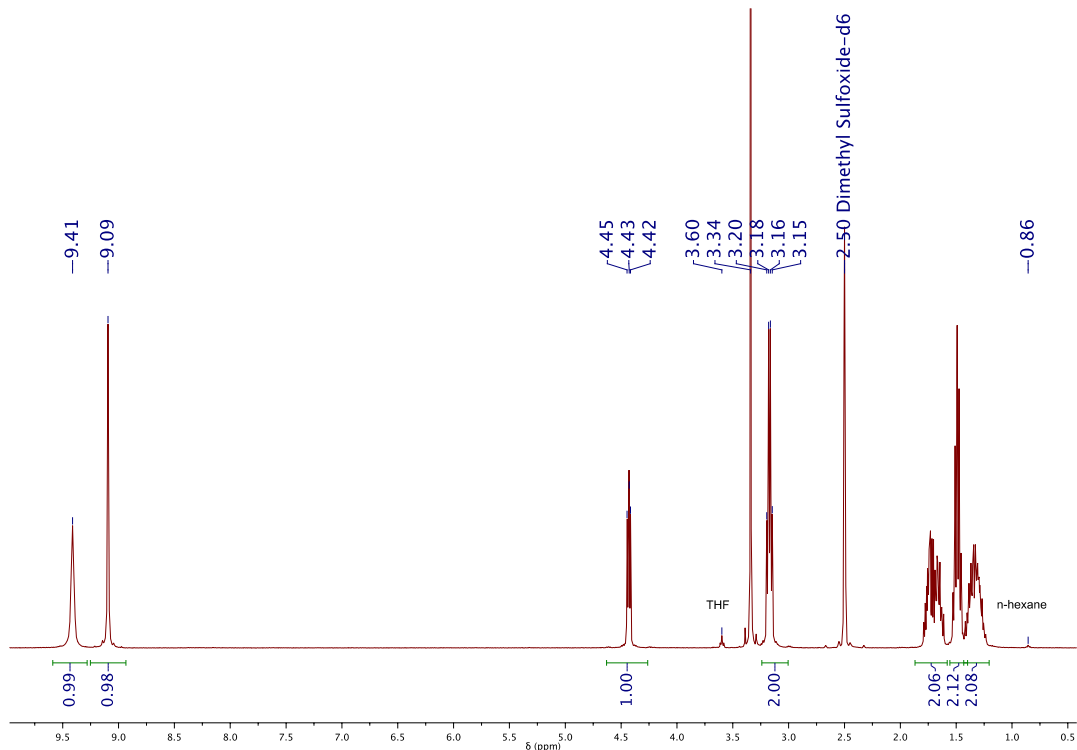


Figure 3: ^1H NMR spectrum of Lys(TFA)NCA in DMSO-d_6 (300 MHz).

1.2 Homopolymers

1.2.1 PSar-NPA 46, 58, 117

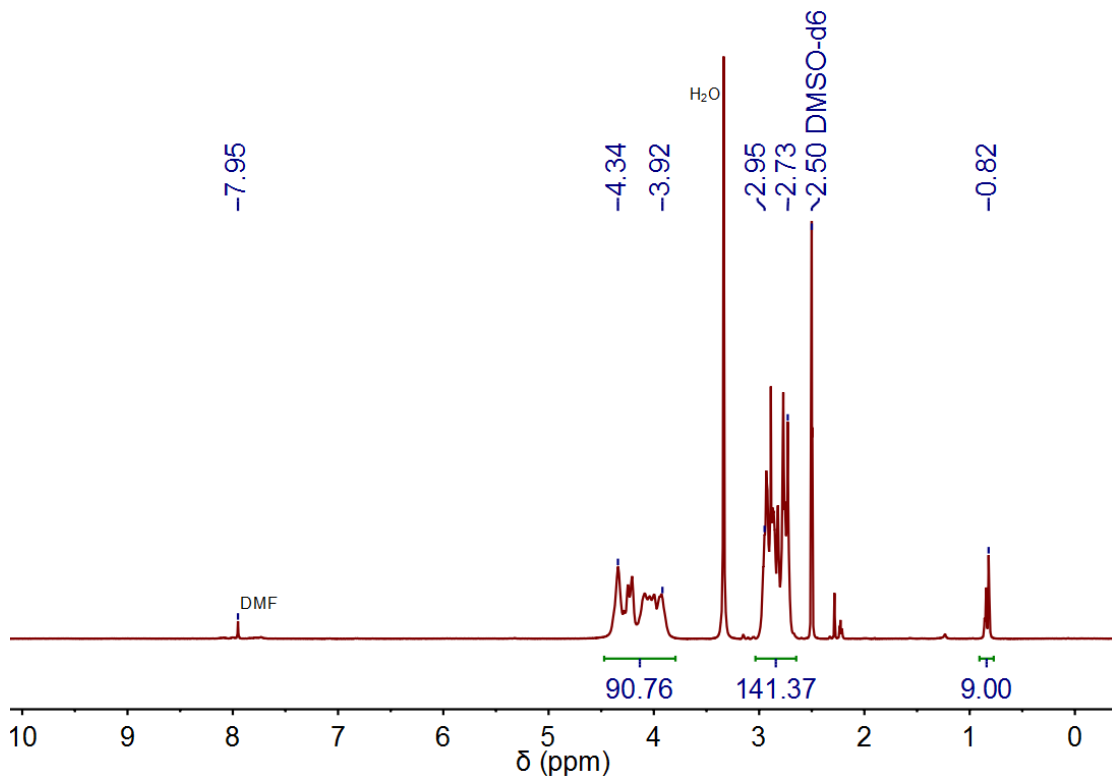


Figure 4: ¹H NMR of PSar-NPA in DMSO-d₆ (400 MHz) ($X_n = 46$).

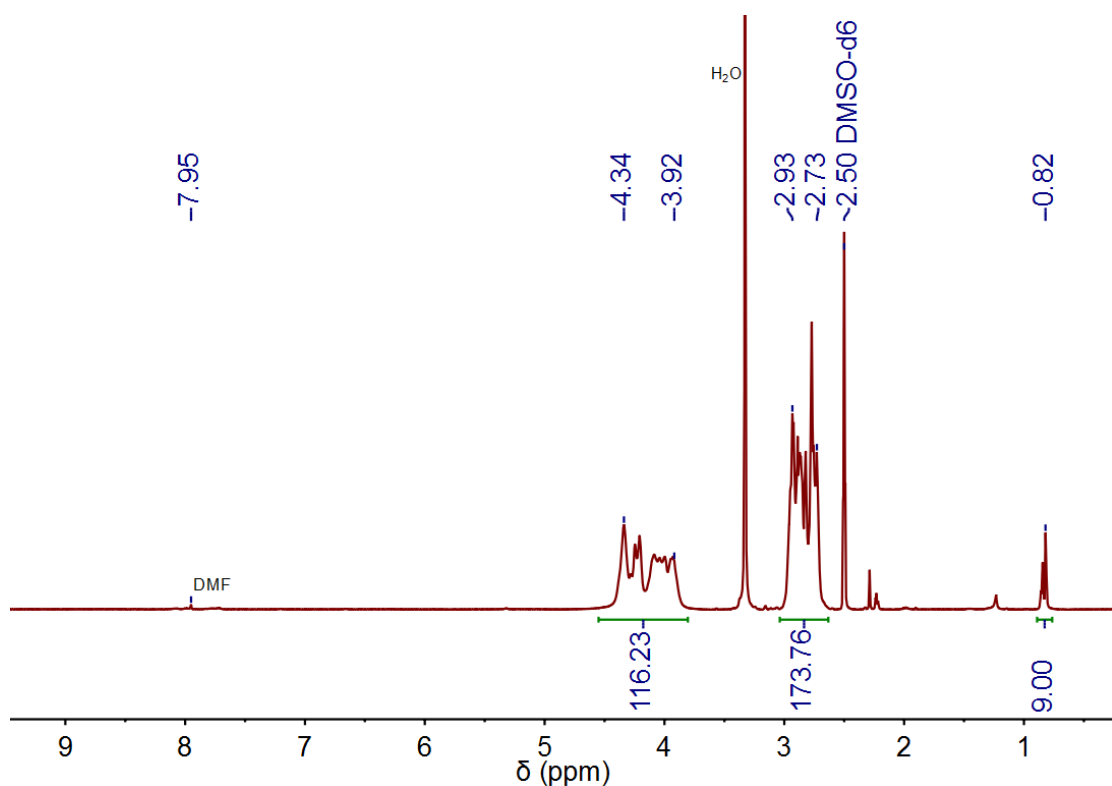


Figure 5: ¹H NMR of PSar-NPA in DMSO-d₆ (400 MHz) ($X_n = 58$).

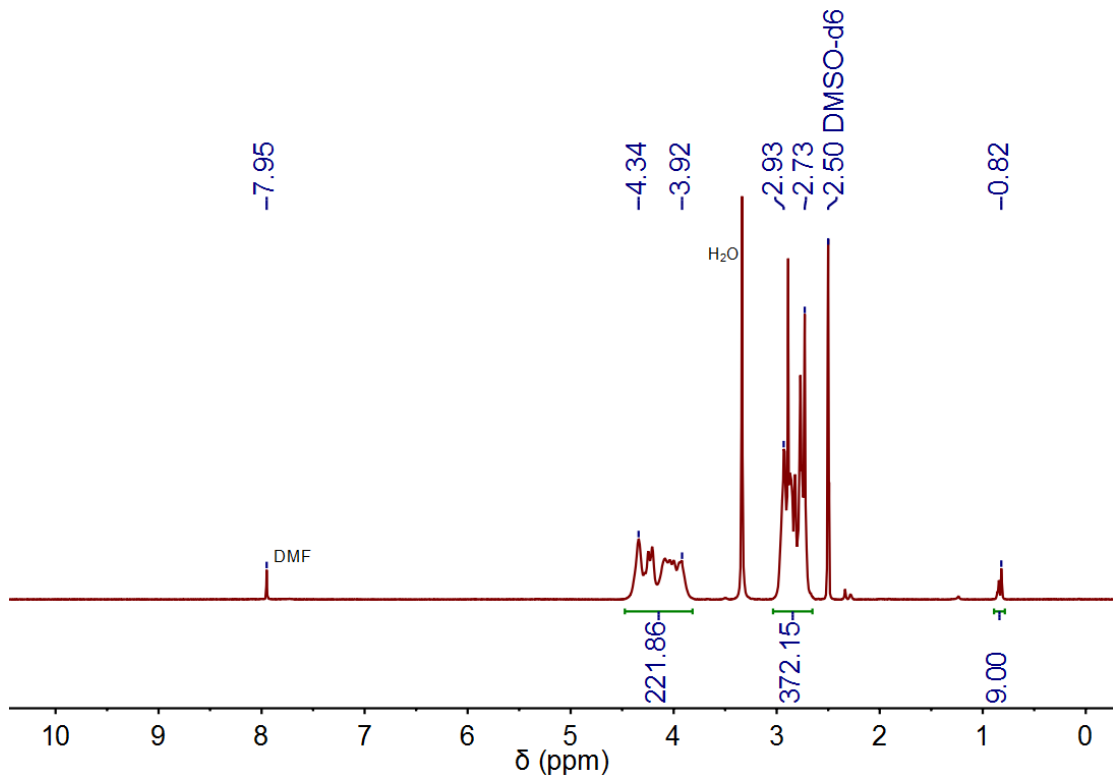


Figure 6: ${}^1\text{H}$ NMR of PSar-NPA in DMSO-d_6 (400 MHz) ($X_n = 117$).

1.2.2 PSar-APA 44, 96

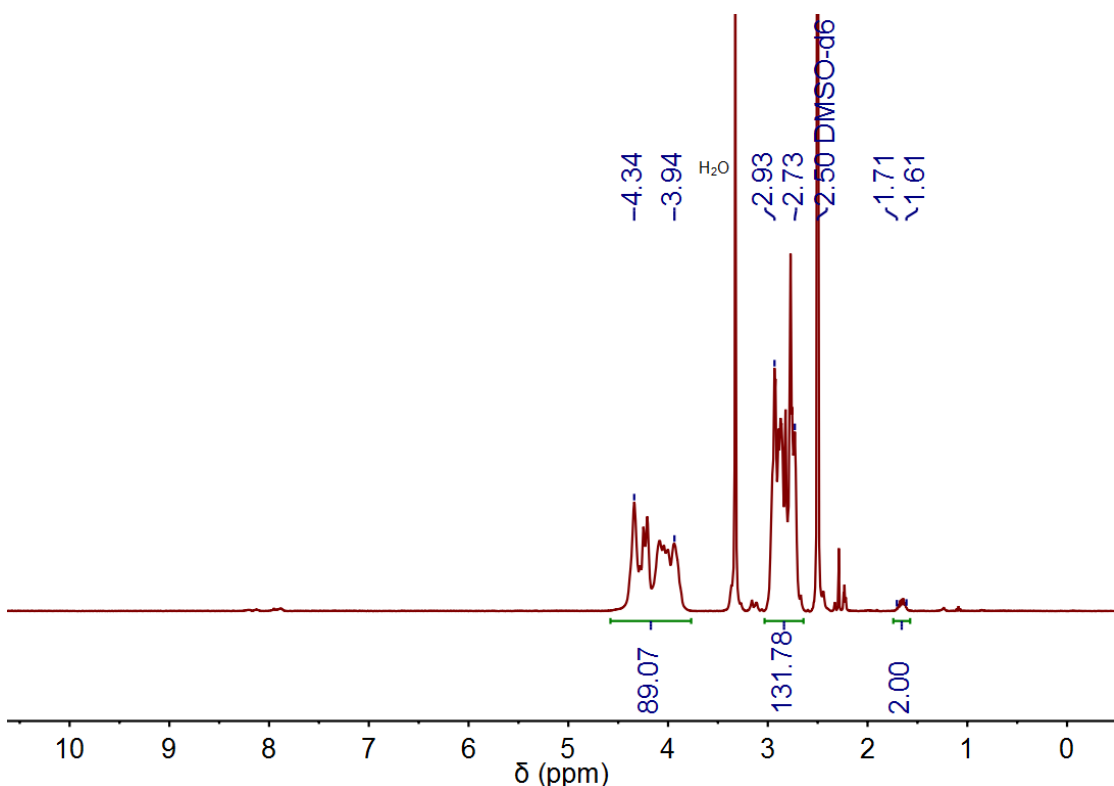


Figure 7: ¹H NMR of PSar-APA in DMSO-d₆ (400 MHz) ($X_n = 44$).

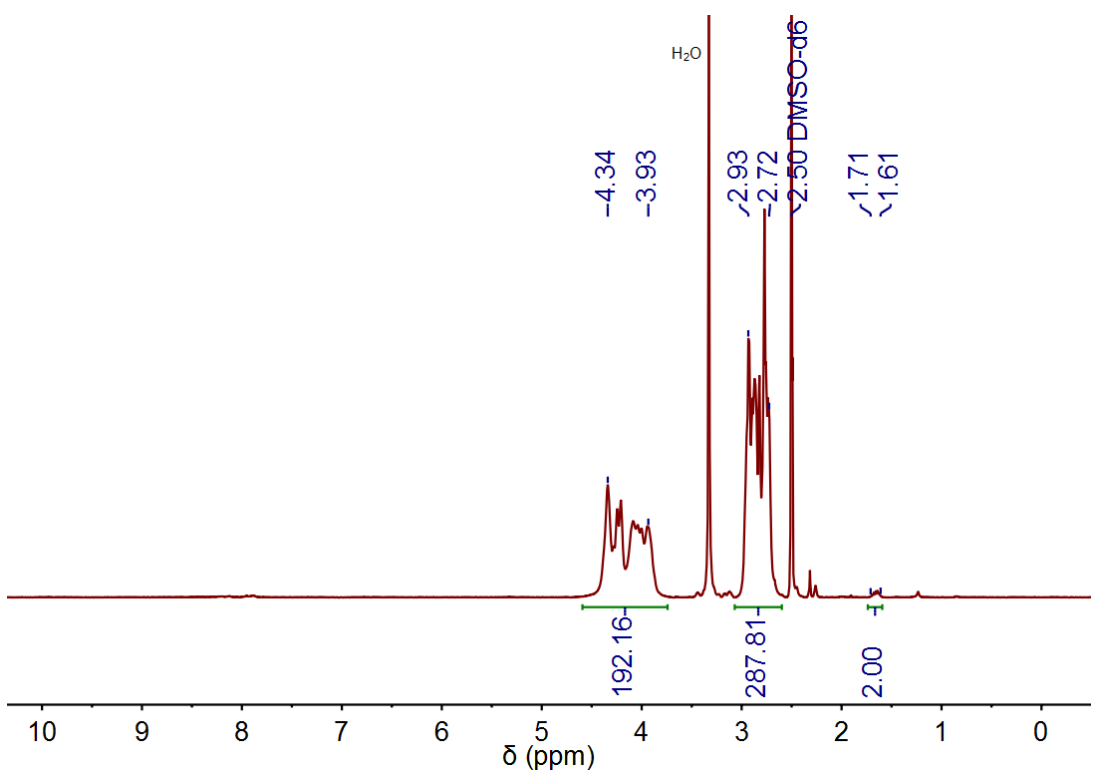


Figure 8: ¹H NMR of PSar-APA in DMSO-d₆ (400 MHz) ($X_n = 96$)

1.2.3 PSar-DBCO 50, 119

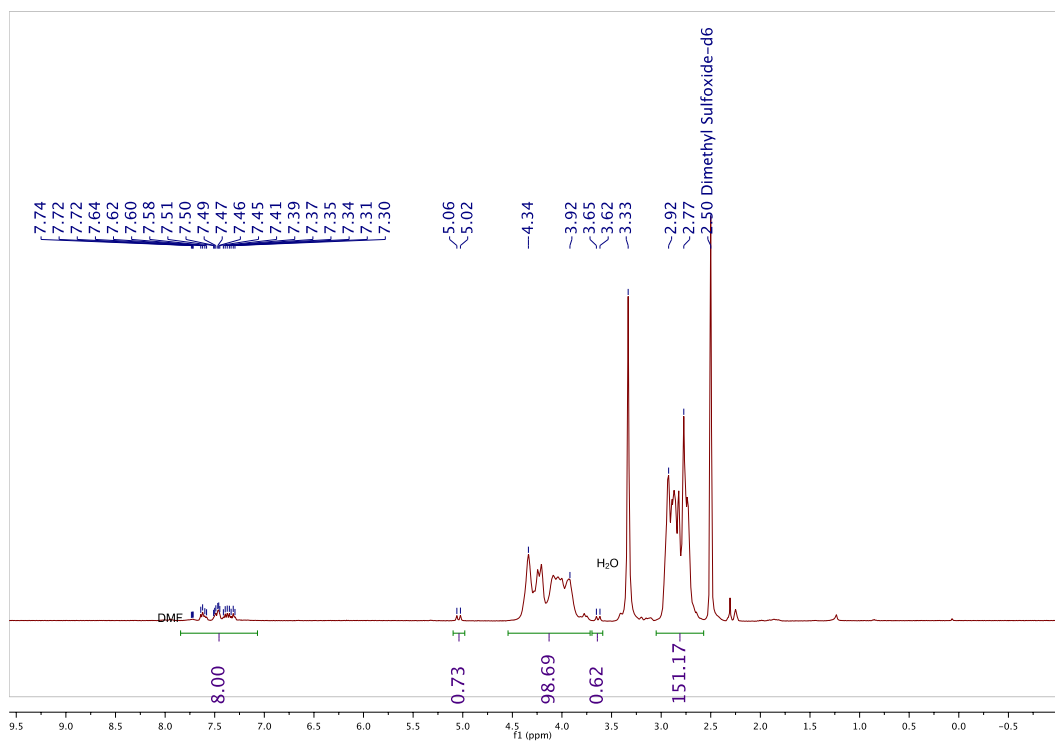


Figure 9: ^1H NMR of PSar-DBCO in DMSO-d_6 (400 MHz) ($X_n = 50$).

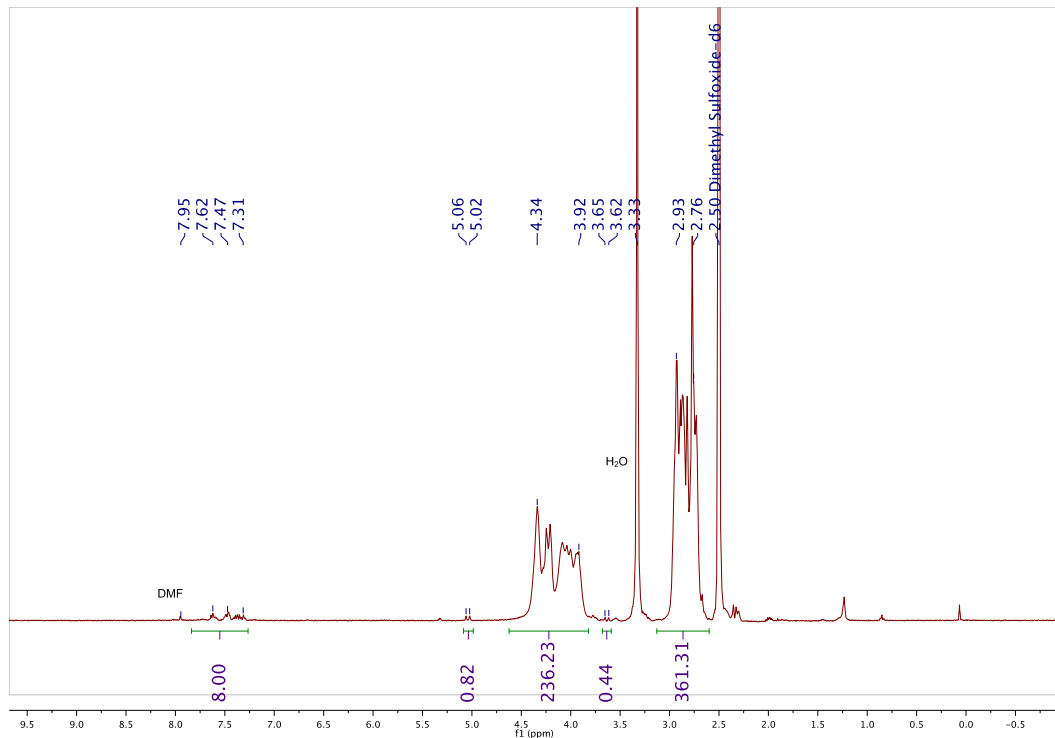


Figure 10: ^1H NMR of PSar-DBCO in DMSO-d_6 (400 MHz) ($X_n = 119$).

1.2.4 PGlu(OBzl)-PA 72, 117

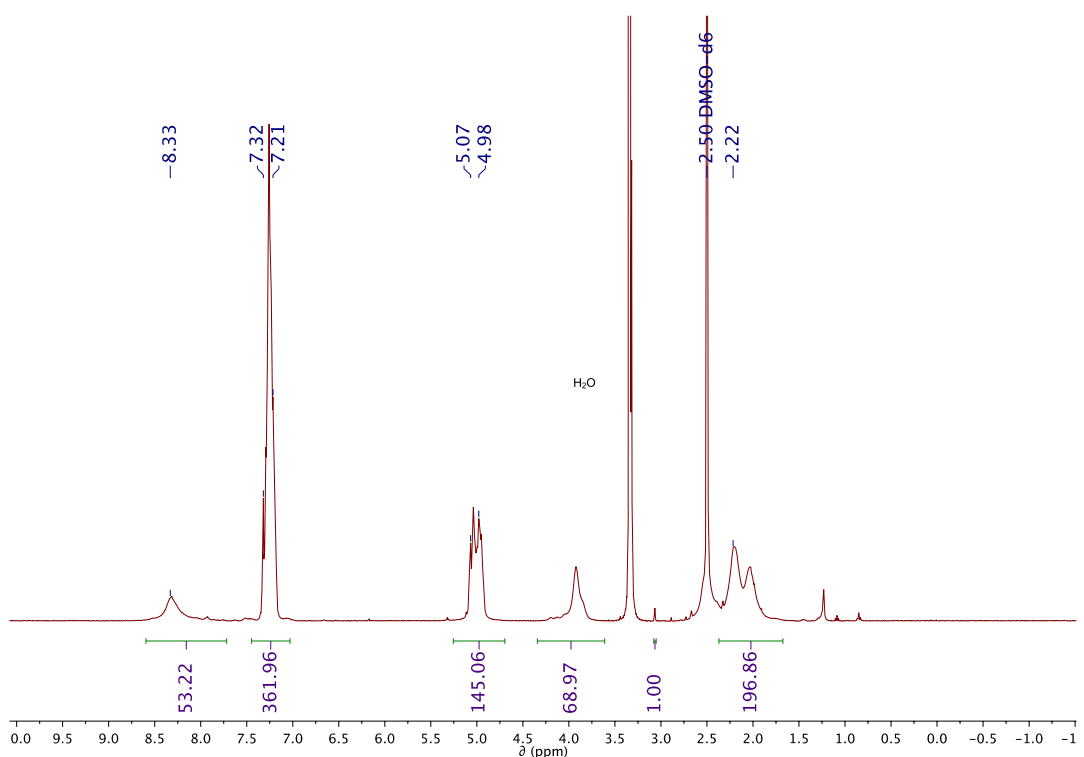


Figure 11: ¹H NMR of PGlu(OBzl)-PA in DMSO-d₆ (400 MHz) ($X_n = 72$).

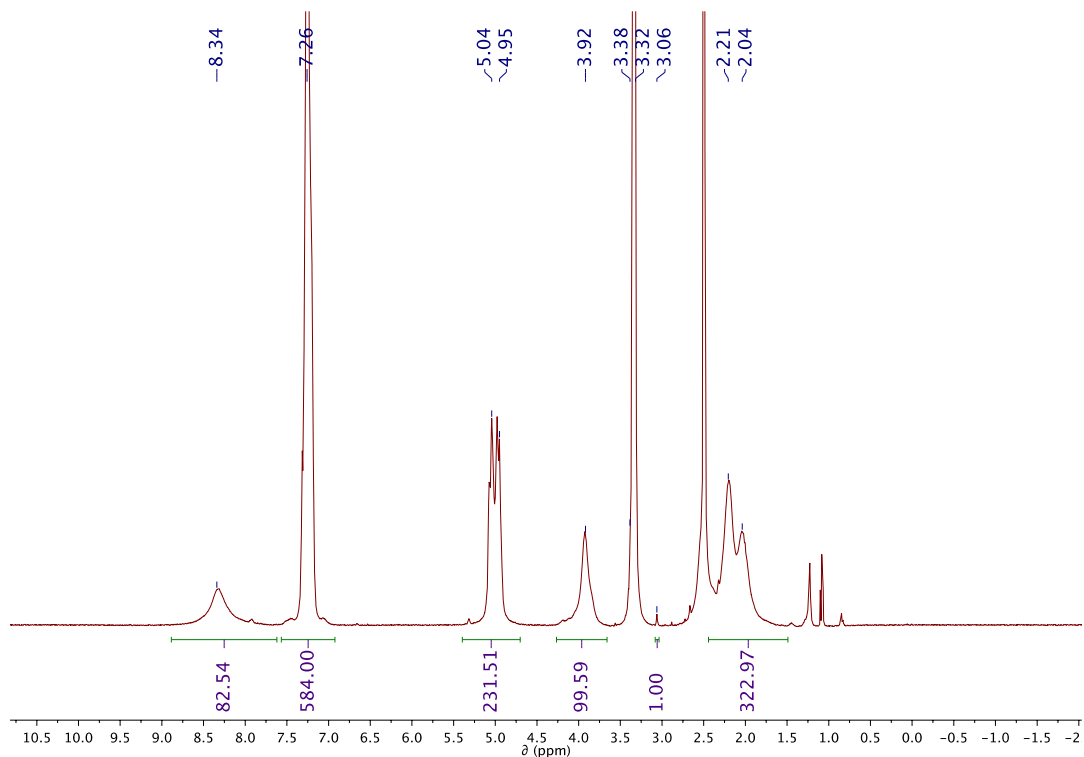


Figure 12: ¹H NMR of PGlu(OBzl)-PA in DMSO-d₆ (400 MHz) ($X_n = 117$).

1.2.5 PGlu(OBzl)-APA 64, 108

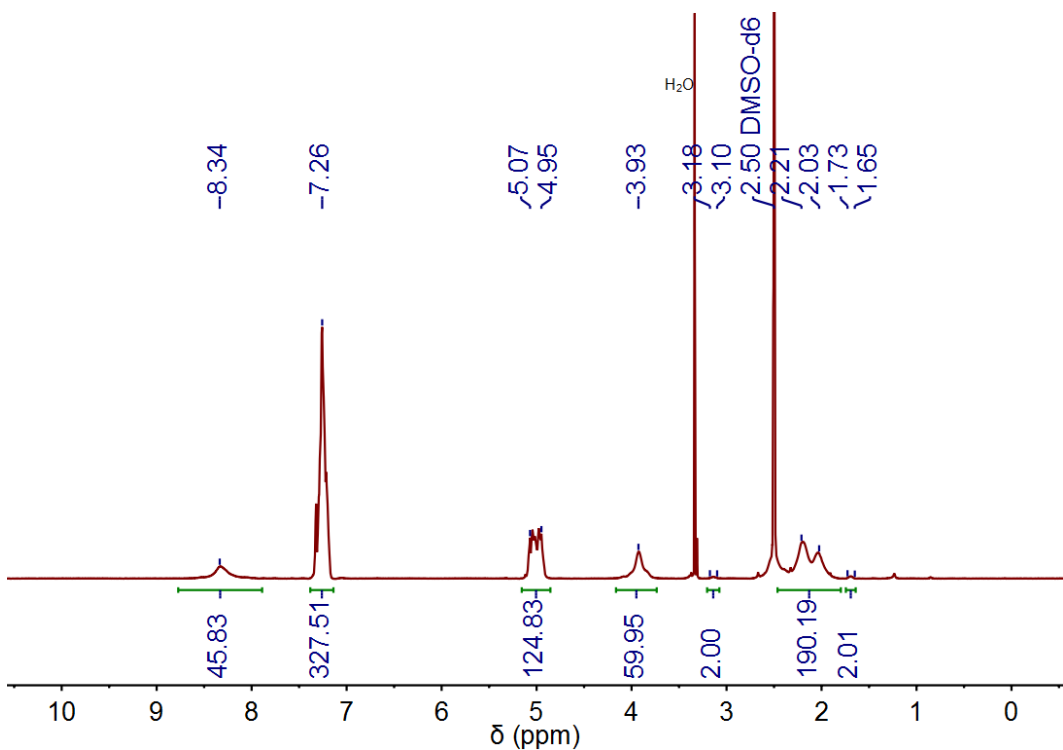


Figure 13: ¹H NMR of PGlu(OBzl)-APA in DMSO-_d6 (400 MHz) (X_n = 64).

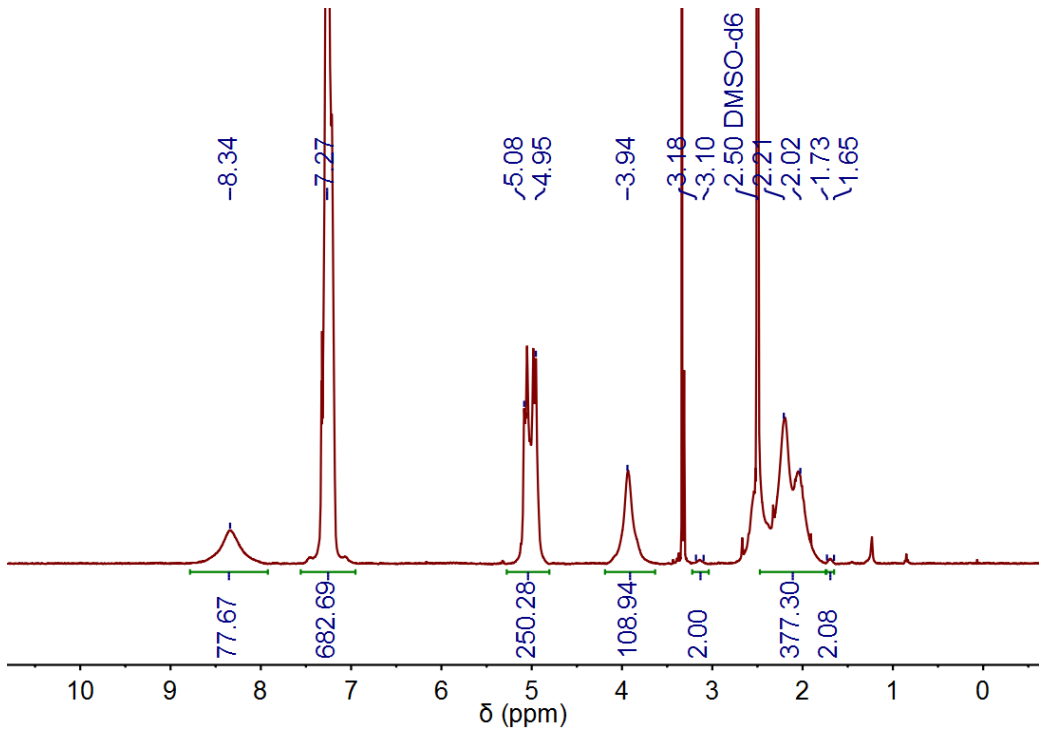
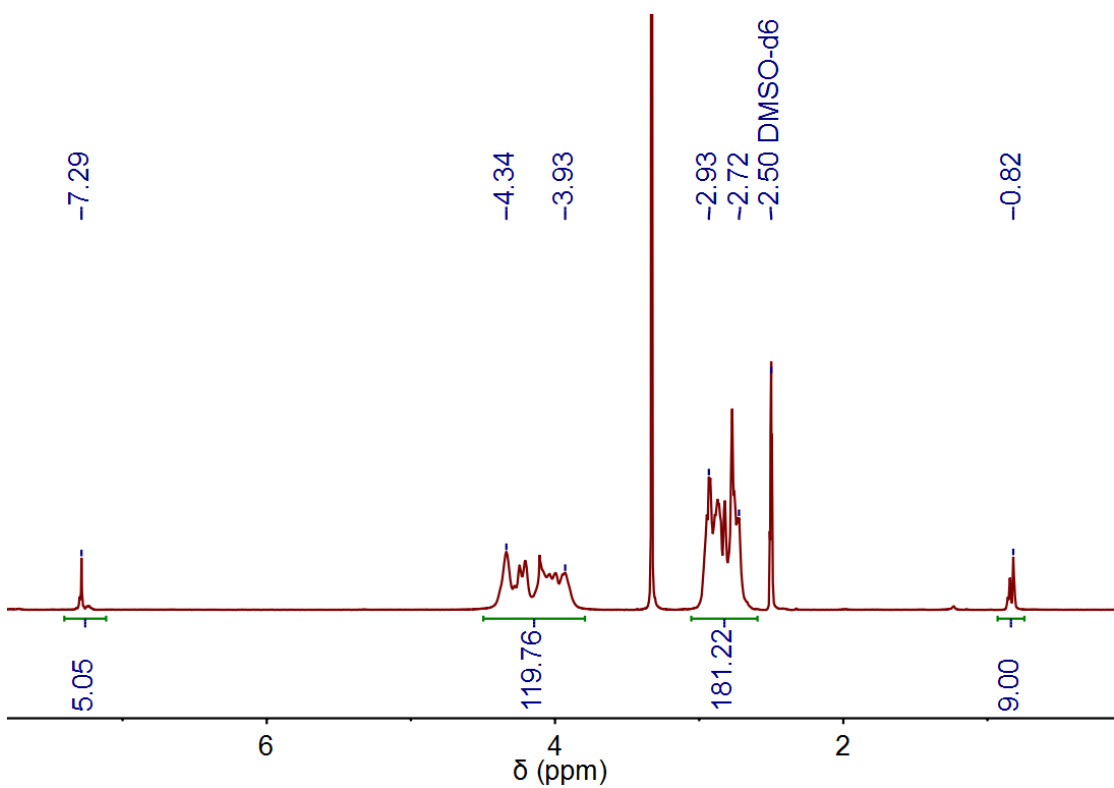
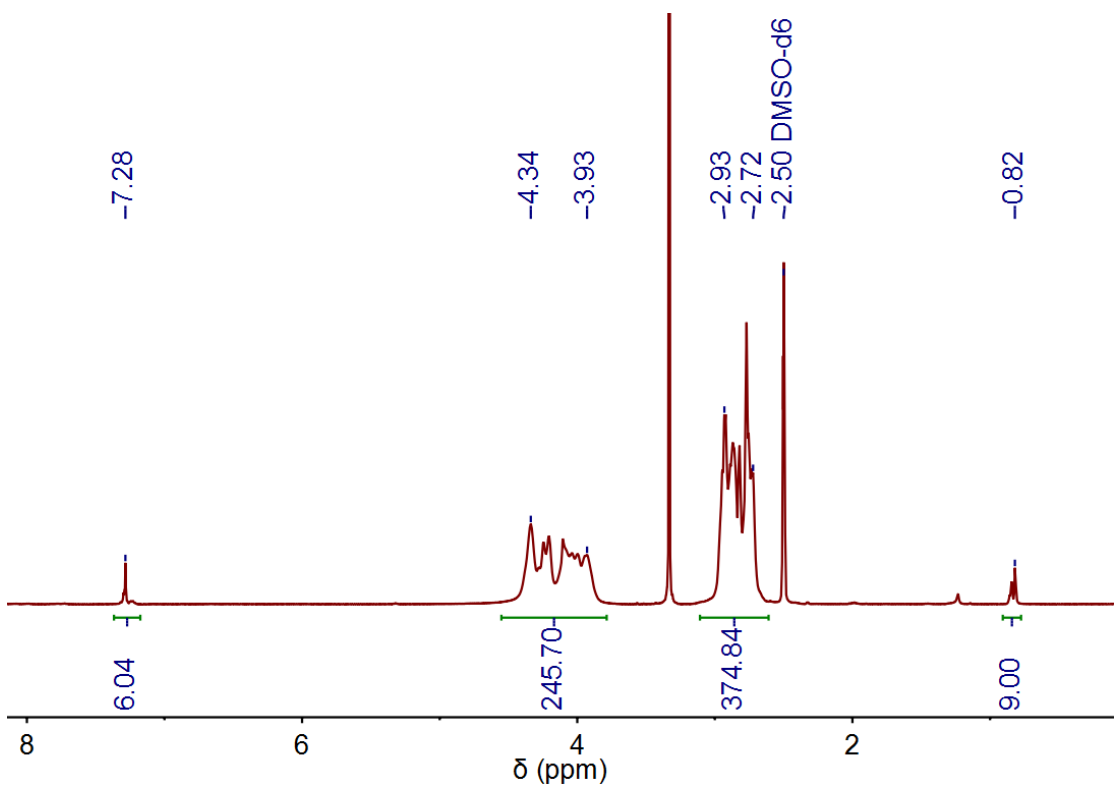


Figure 14: ¹H NMR of PGlu(OBzl)-APA in DMSO-_d6 (400 MHz) (X_n = 108).

1.2.6 PSar-NPA with S-Benzylthiosuccinate modification

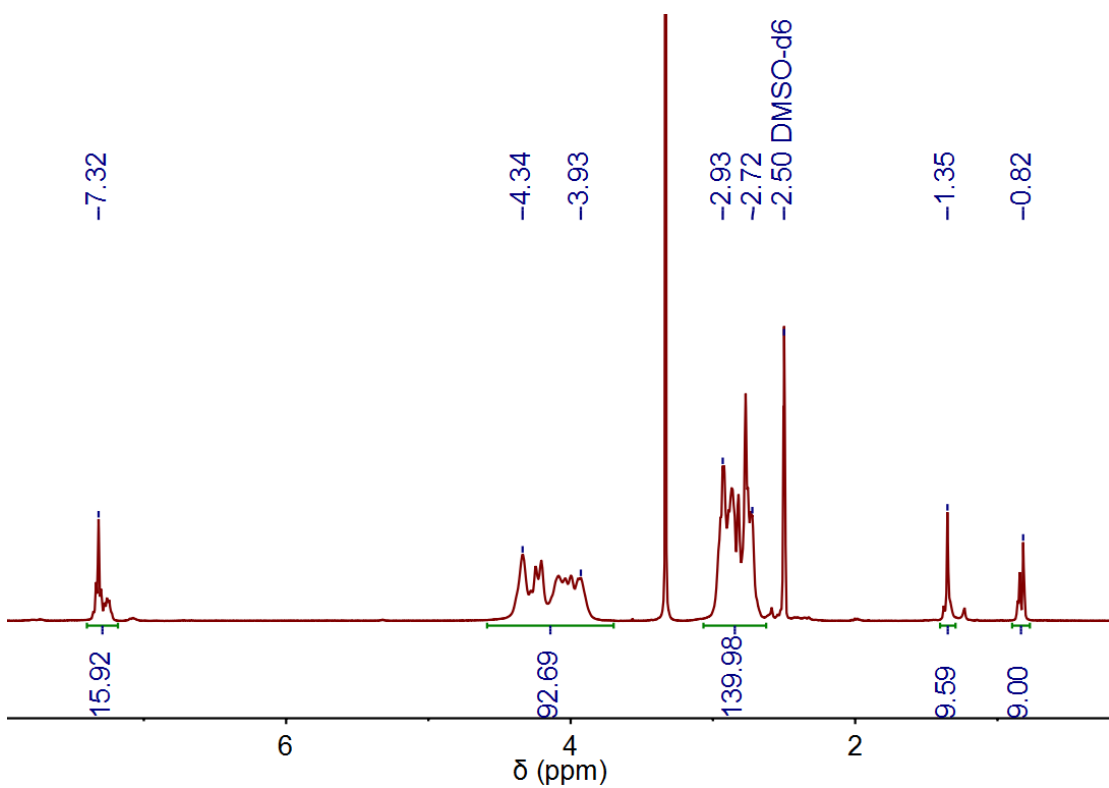


FigureX: ¹H NMR of PSar-NPA with S-benzylthiosuccinate (quant.) in DMSO-d₆ (400 MHz) (X_n = 60).

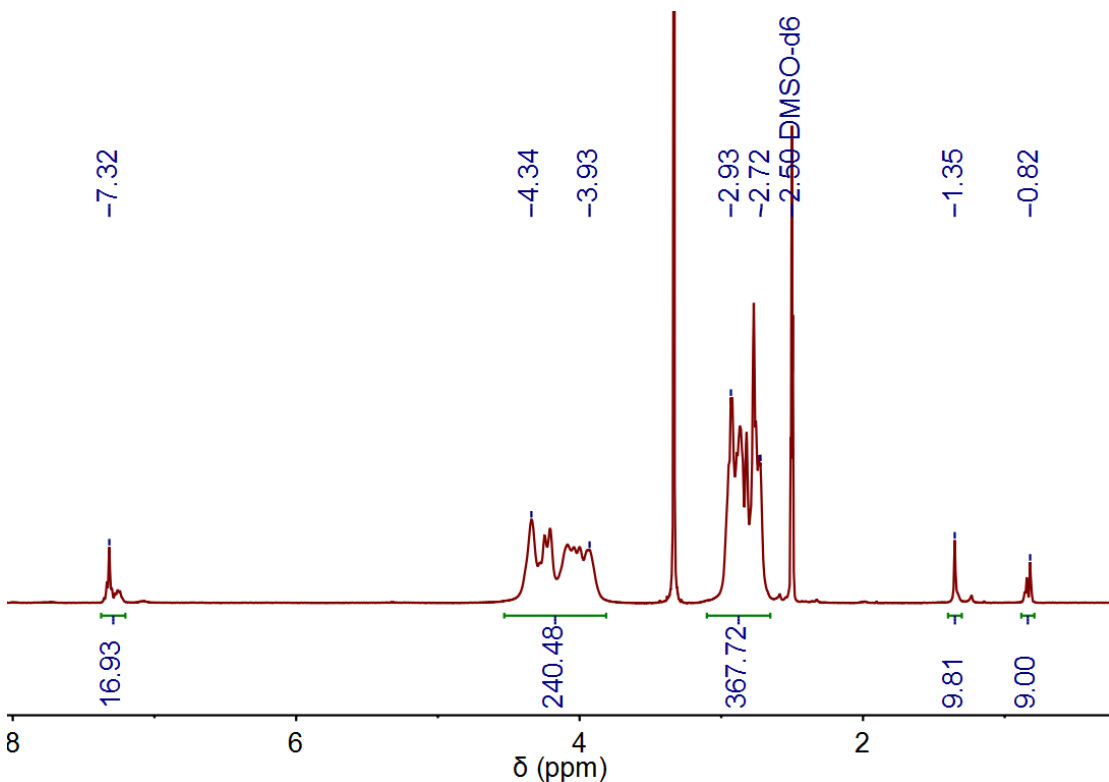


FigureX: ¹H NMR of PSar-NPA with S-benzylthiosuccinate (quant.) in DMSO-d₆ (400 MHz) (X_n = 124).

1.2.7. PSar-NPA with Boc-Cys(Trt) modification

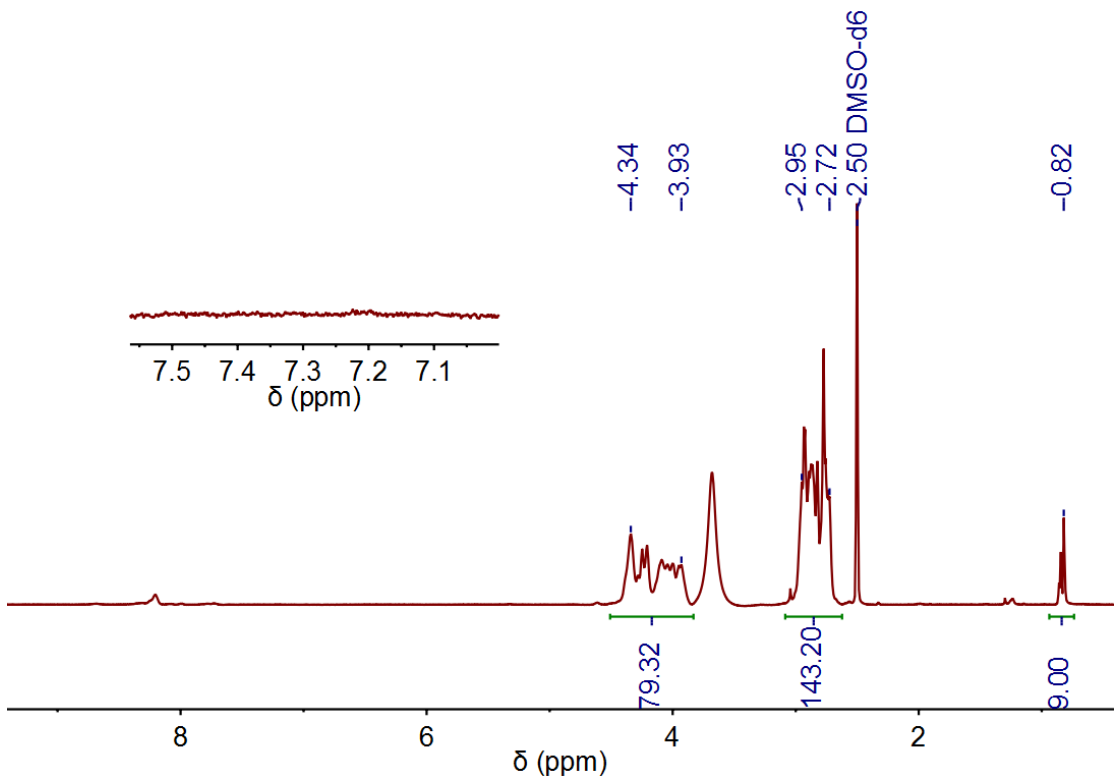


FigureX: ¹H NMR of PSar-NPA with Boc-L-Cys(Trt) end group modification (quant.) in DMSO-d₆ (400 MHz) ($X_n = 46$).

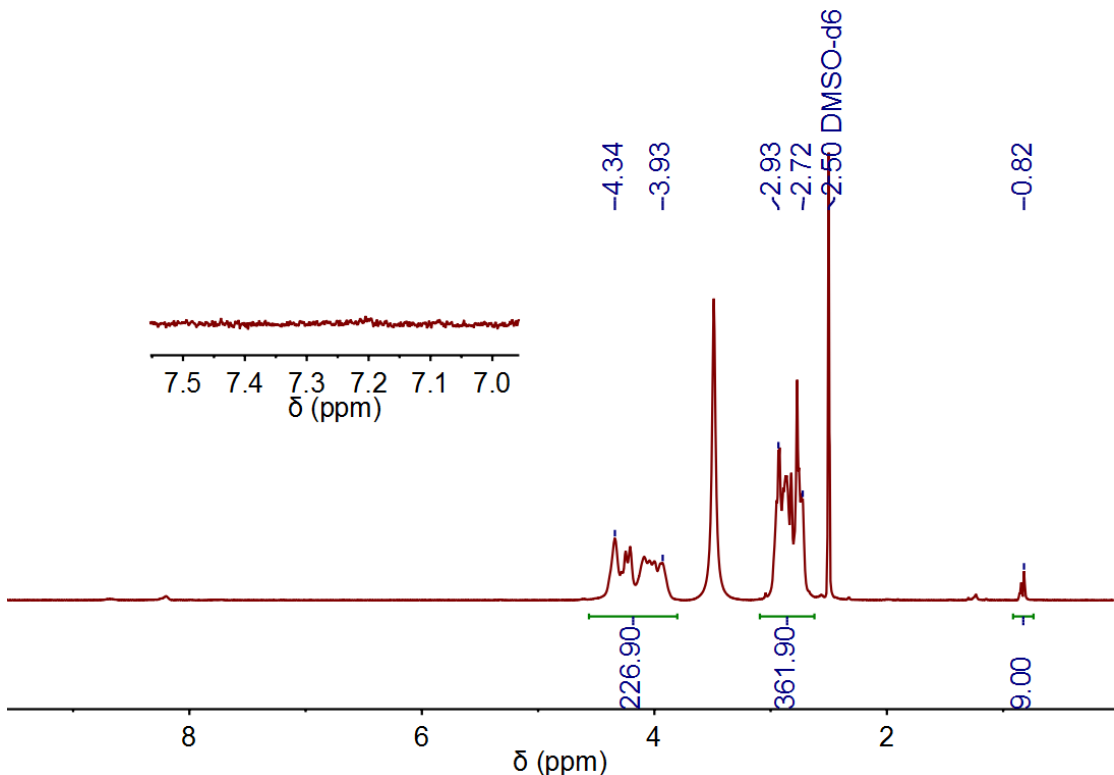


FigureX: ¹H NMR of PSar-NPA with Boc-L-Cys(Trt) end group modification (quant.) in DMSO-d₆ (400 MHz) ($X_n = 121$).

1.2.8 PSar-Cys (after deprotection in TFA)



FigureX: ¹H NMR of PSar-Cys after deprotection in TFA measured in DMSO-d₆ (400 MHz) ($X_n = 44$).



FigureX: ¹H NMR of PSar-Cys after deprotection in TFA measured in DMSO-d₆ (400 MHz) ($X_n = 117$).

1.2.9 PLys(TFA)-NPA with Boc-Cys(Trt) modification

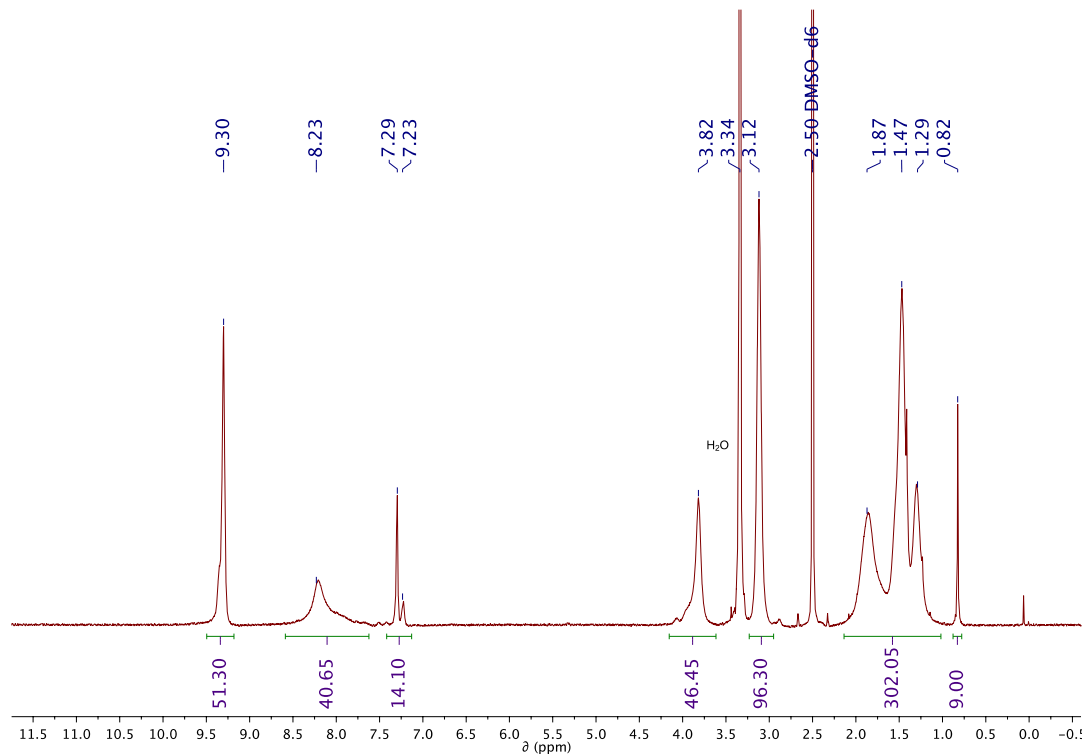


Figure 15: ¹H NMR of PLys(TFA)-NPA with Boc-L-Cys(Trt) end group modification (94%) in DMSO-d₆ (400 MHz) ($X_n = 49$).

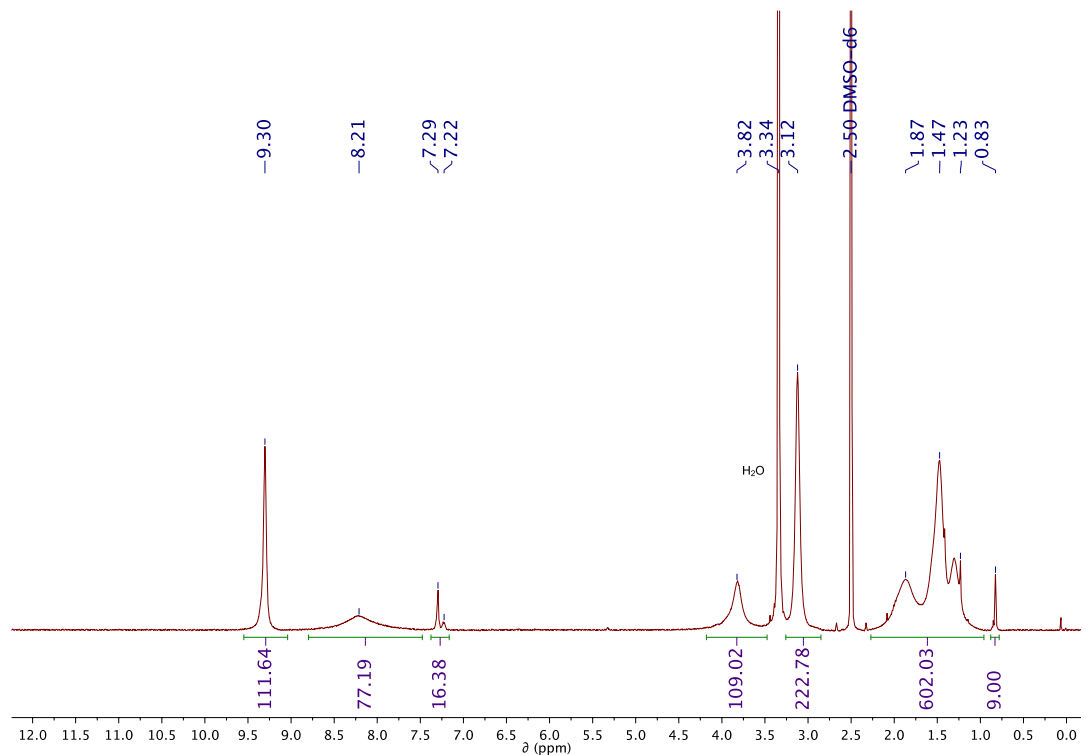


Figure 16: ¹H NMR of PLys(TFA)-NPA with Boc-L-Cys(Trt) end group modification (quantitative) in DMSO-d₆ (400 MHz) ($X_n = 111$).

1.2.[10](#) PLys(TFA)-Cys (after deprotection in TFA)

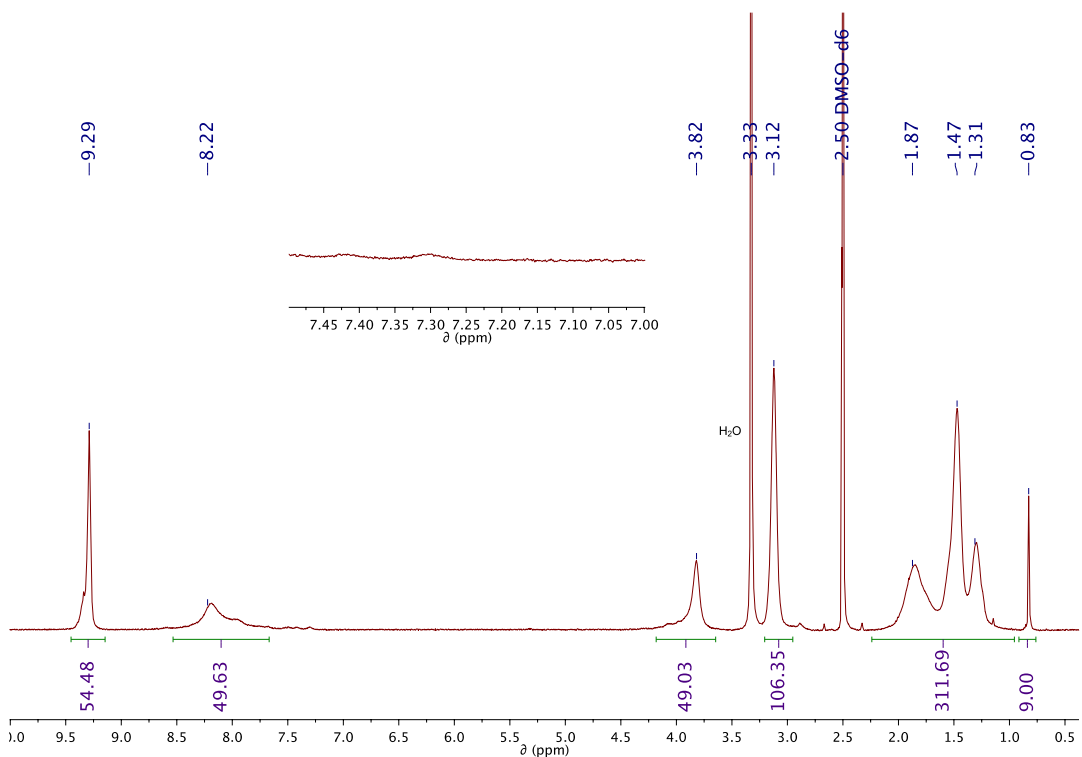


Figure [17](#): ¹H NMR of PLys(TFA)-Cys after deprotection in TFA measured in DMSO-d₆ (400 MHz) ($X_n = 53$).

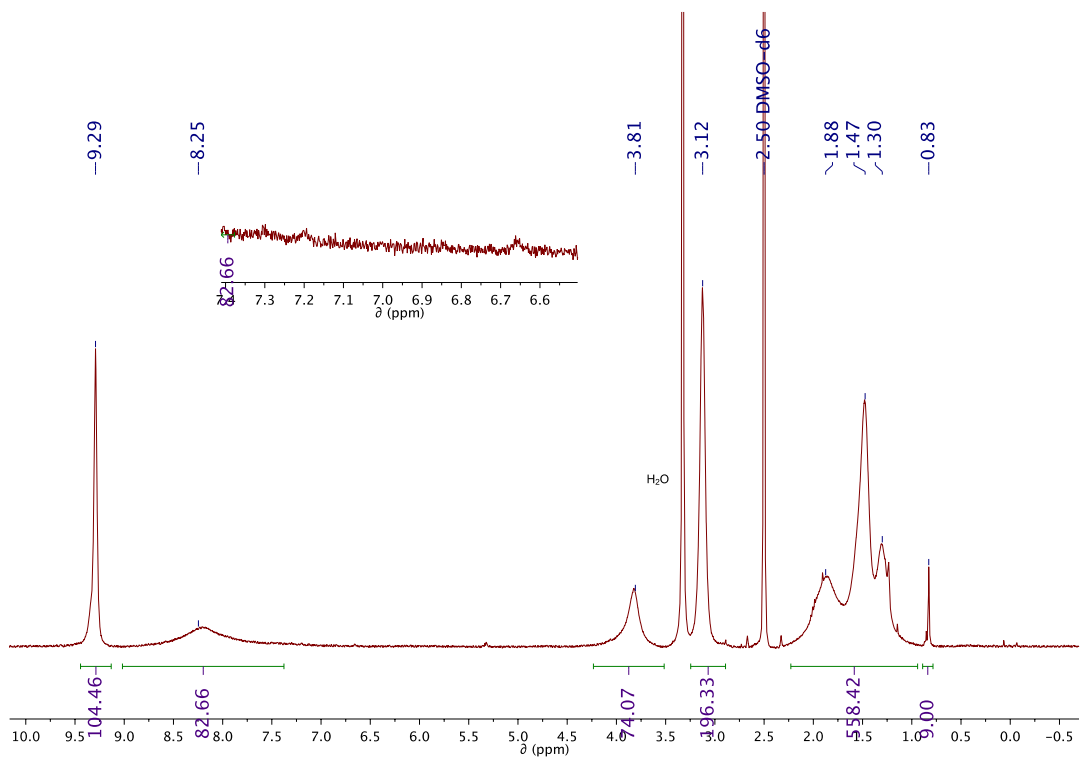


Figure [18](#): ¹H NMR of PLys(TFA)-Cys after deprotection in TFA measured in DMSO-d₆ (400 MHz) ($X_n = 99$).

1.3 S-Benzylthiosuccinic acid

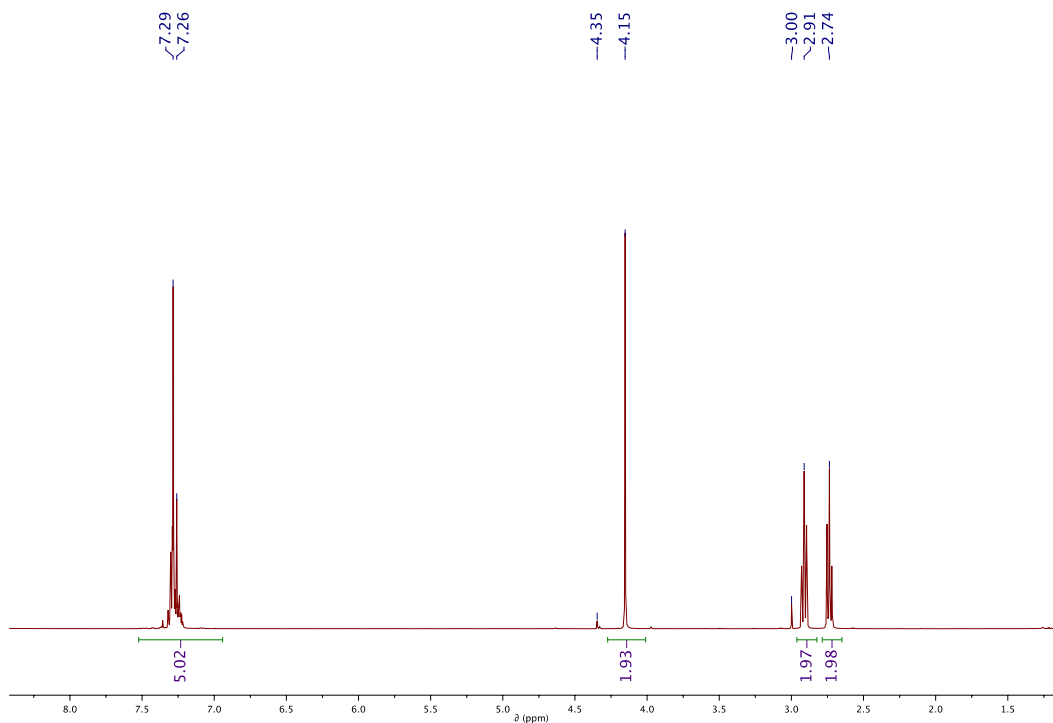


Figure 19: ¹H NMR spectrum of S-benzylthiosuccinic acid in CDCl_3 (400 MHz).

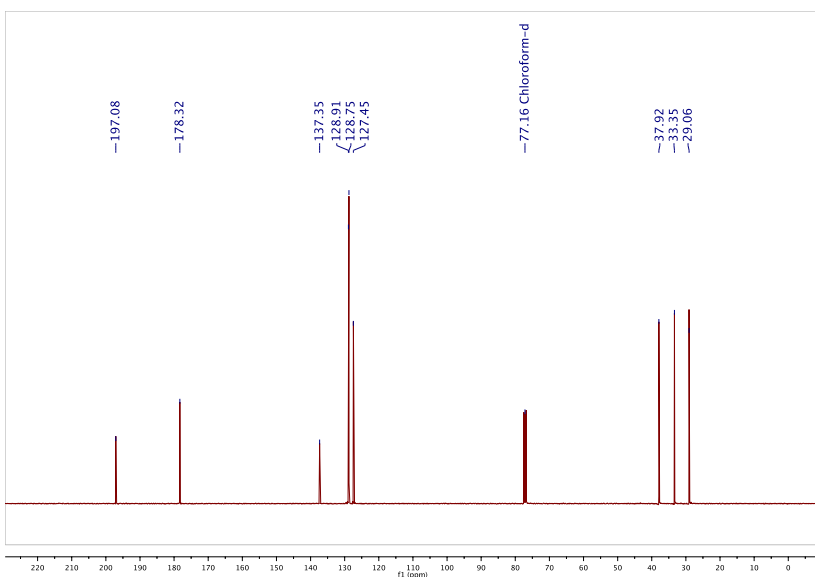


Figure 20: ¹³C NMR spectrum of S-benzylthiosuccinic acid in CDCl_3 (100 MHz).

1.4 3-Azido-1-aminopropane

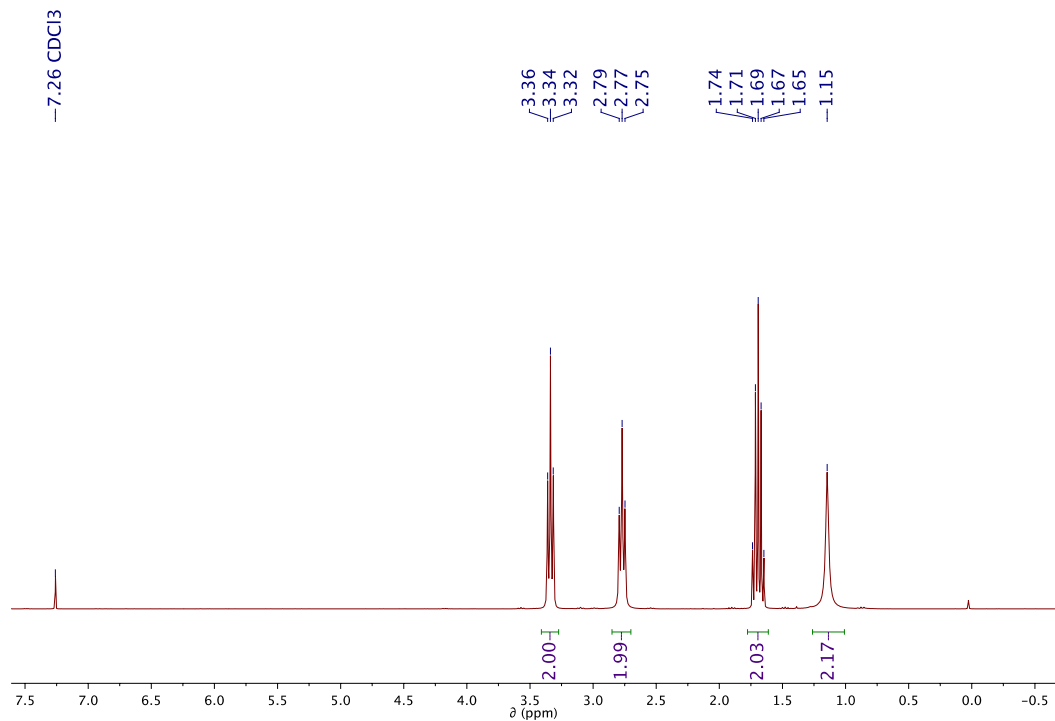


Figure 21: ^1H NMR spectrum of 1-azido-3-aminopropane in CDCl_3 (300 MHz).

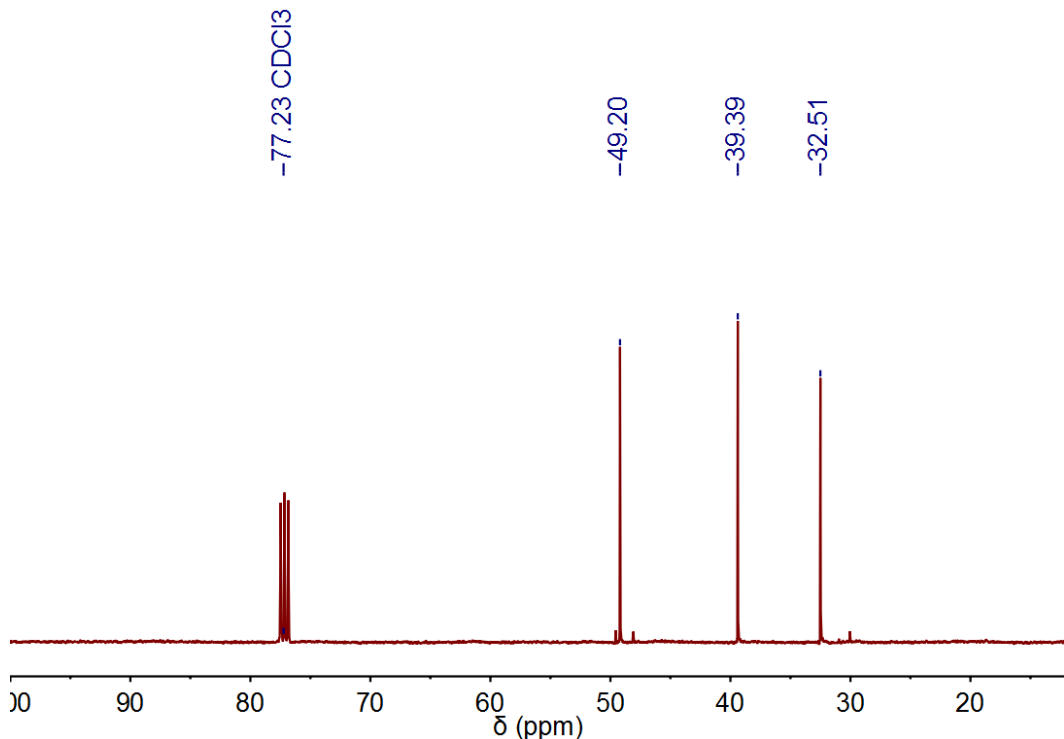


Figure 22: ^{13}C NMR spectrum of 1-azido-3-amino propane in CDCl_3 (100 MHz).

1.5 NMR of CuAAC ligation short

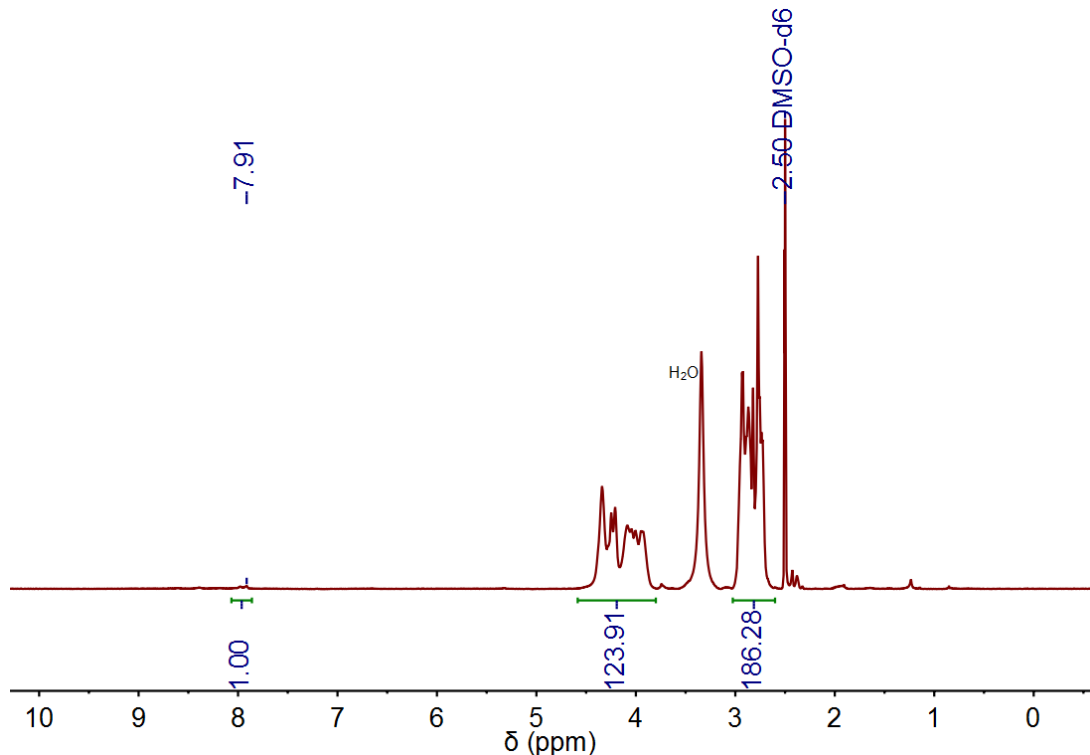


Figure 23: ¹H NMR of CuAAC ligation product; hydrophilic, short.

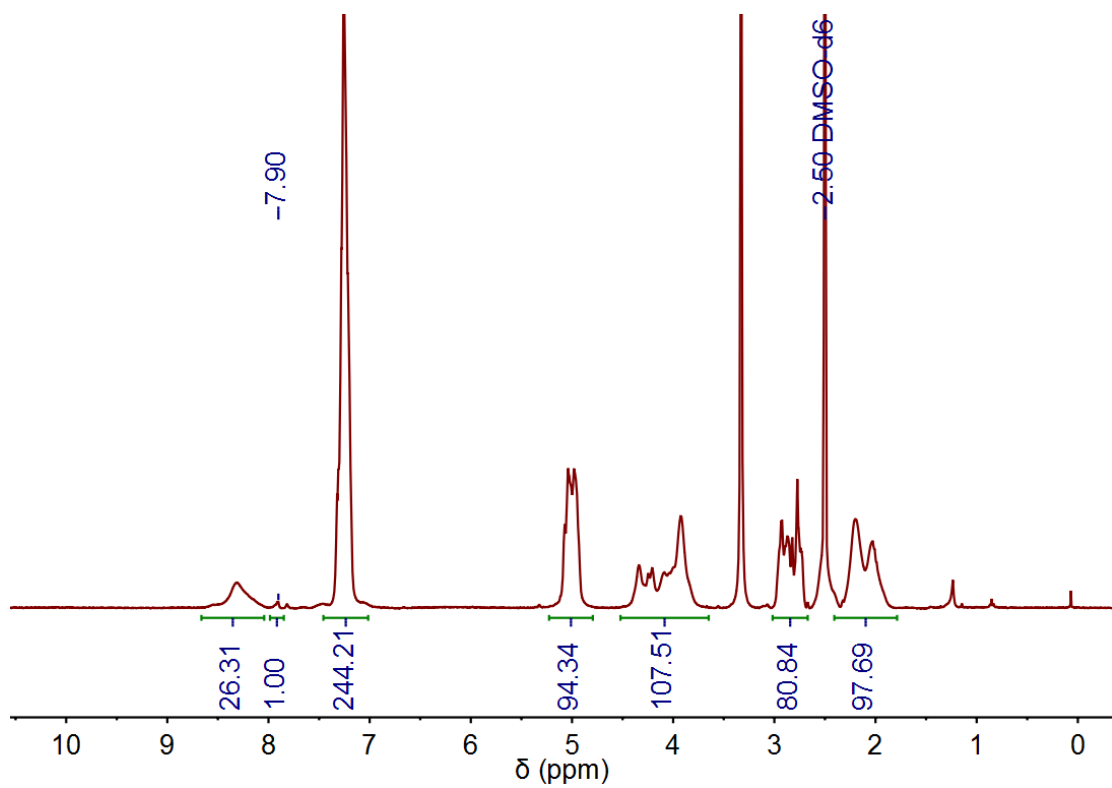


Figure 24: ¹H NMR of CuAAC ligation product; amphiphilic, short.

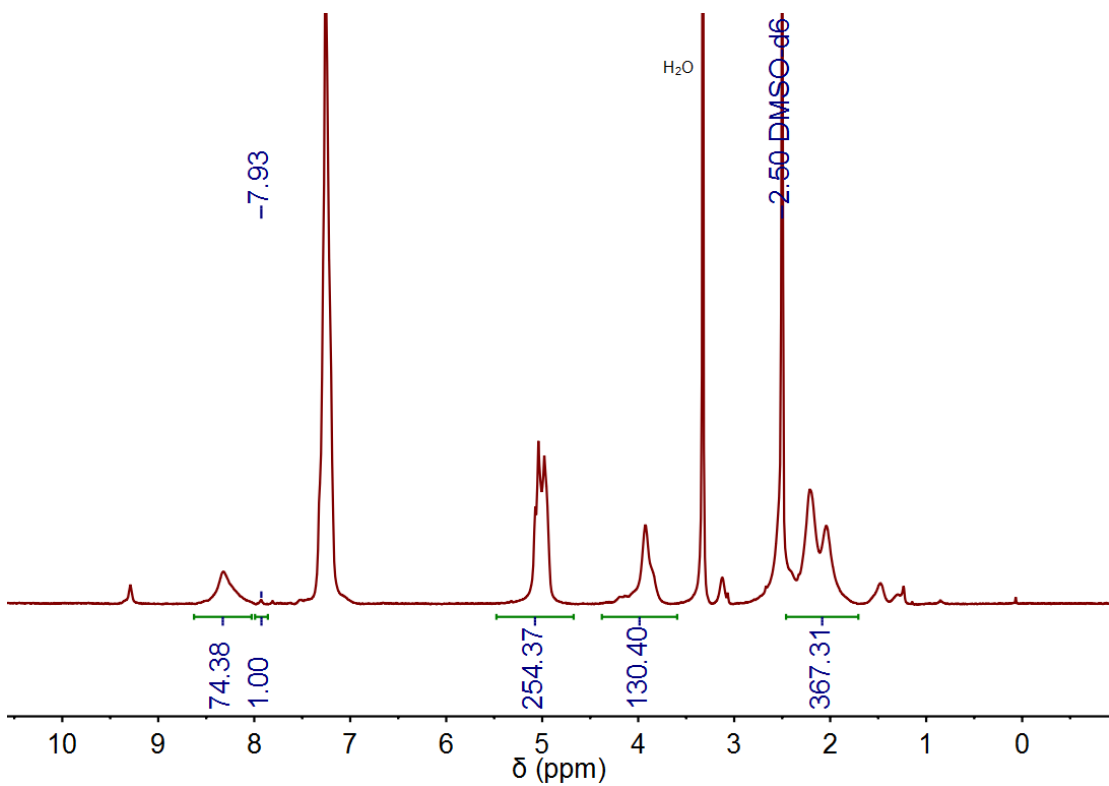


Figure 25: ^1H NMR of CuAAC ligation product; hydrophobic, short.

1.6 ^1H NMR DOSY spectrum of mixture of unfunctionalized PSar and TCR CP

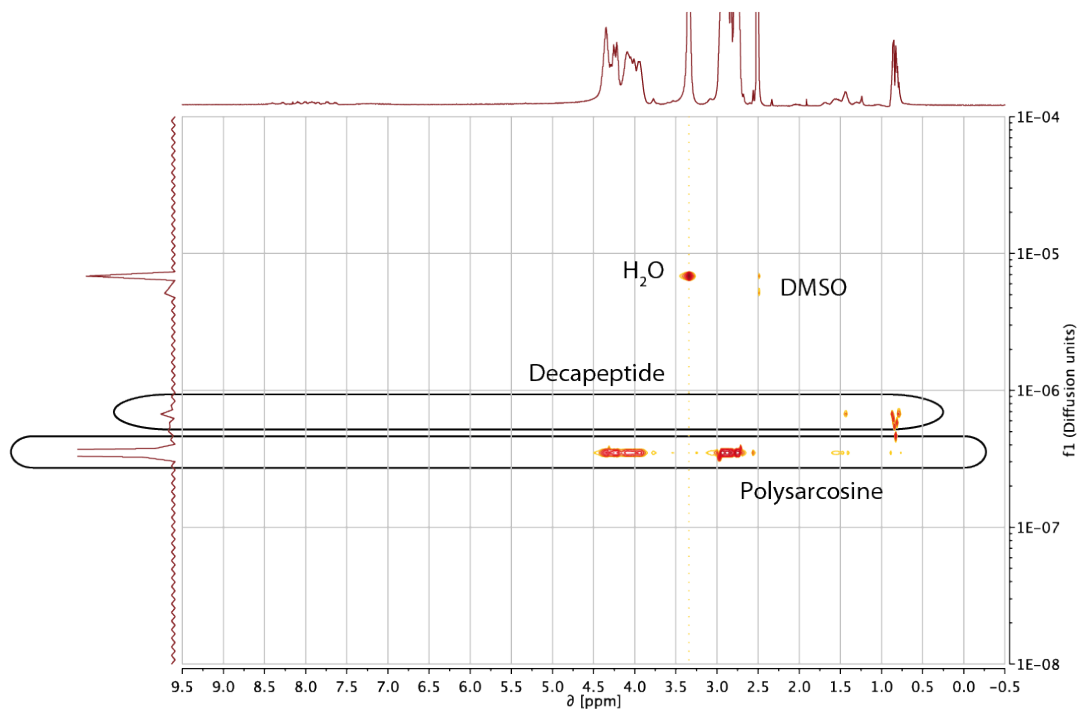


Figure 26: ^1H NMR DOSY spectrum of mixture between unfunctionalized neopenylamine initiated PSar ($X_n = 113$) and TCR CP.

2. FT-IR Spectra of Azide-functionalized Homopolymers

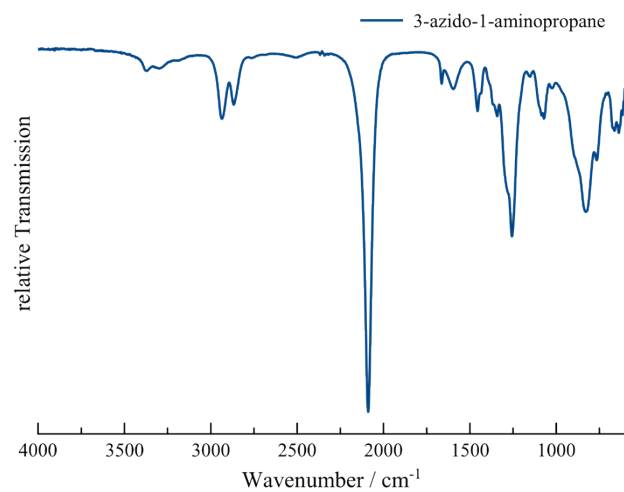


Figure 27: FT-IR spectrum of 3-azido-1-aminopropylamine (APA), $\nu(\text{azide}) = 2088.5 \text{ cm}^{-1}$.

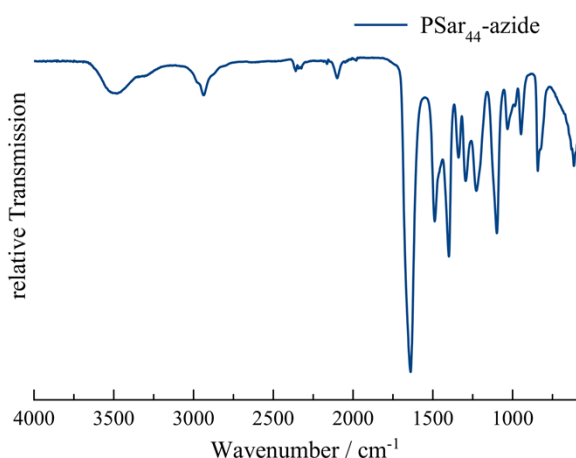


Figure 28: FT-IR spectrum of PSar-APA for proof of azide functionality $\nu(\text{azide}) = 2099.1 \text{ cm}^{-1}$ (PSar₄₄-APA).

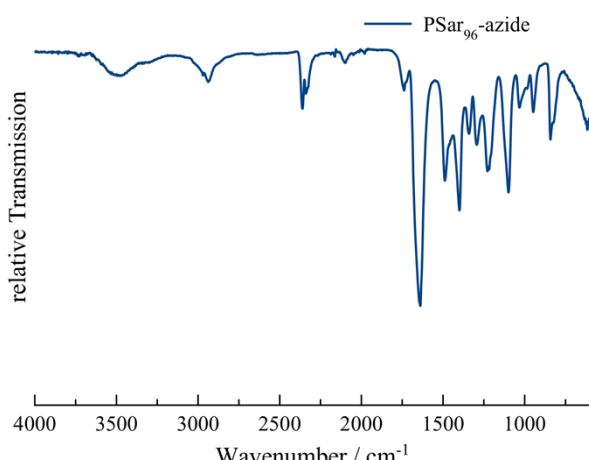


Figure 29: FT-IR spectrum of PSar-APA for proof of azide functionality $\nu(\text{azide}) = 2098.2 \text{ cm}^{-1}$ (PSar₉₆-APA).

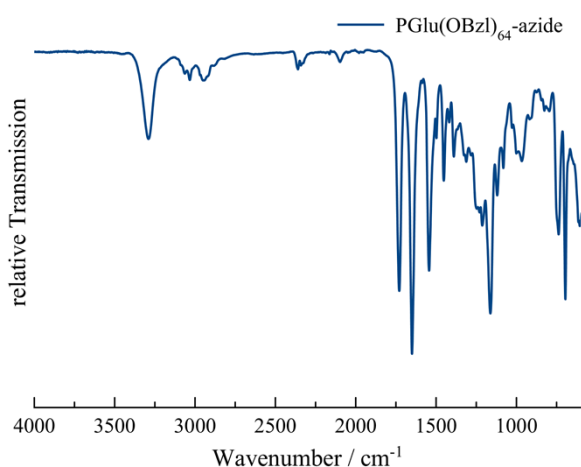


Figure 30: FT-IR spectrum of PGlu(OBzl)-APA for proof of azide functionality $\nu(\text{azide}) = 2097.2 \text{ cm}^{-1}$ ($\text{PGlu(OBzl)}_{64}\text{-APA}$).

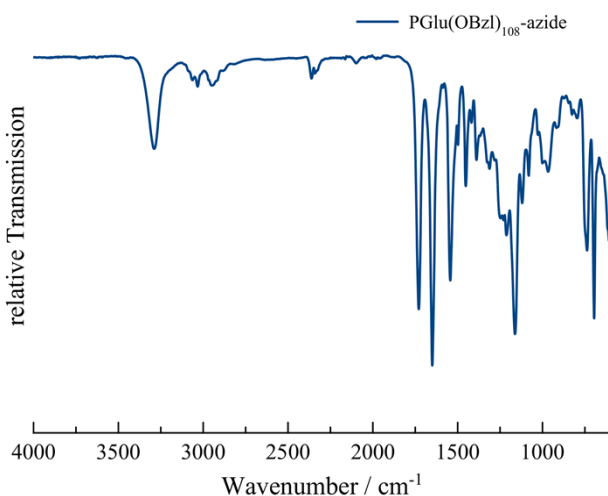


Figure 31: FT-IR spectrum of PGlu(OBzl)-APA for proof of azide functionality $\nu(\text{azide}) = 2097.2 \text{ cm}^{-1}$ ($\text{PGlu(OBzl)}_{108}\text{-APA}$).

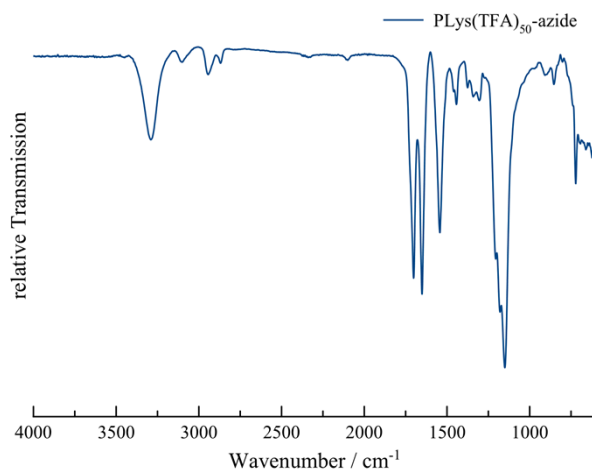


Figure 32: FT-IR spectrum of PLys(TFA)-APA for proof of azide functionality $\nu(\text{azide}) = 2103.0 \text{ cm}^{-1}$ ($\text{PLys(TFA)}_{50}\text{-APA}$).

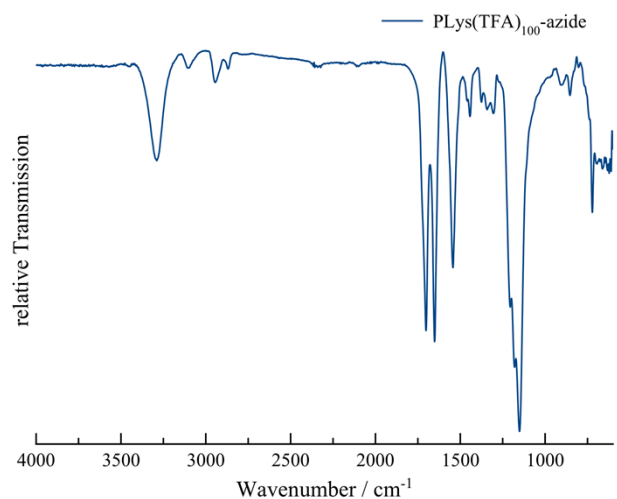


Figure 33: FT-IR spectrum of PLys(TFA)-APA for proof of azide functionality $\nu(\text{azide}) = 2106.9 \text{ cm}^{-1}$ (PLys(TFA)₁₀₀-APA).

3. HFIP GPC Data of Ligation Products and Homopolymers

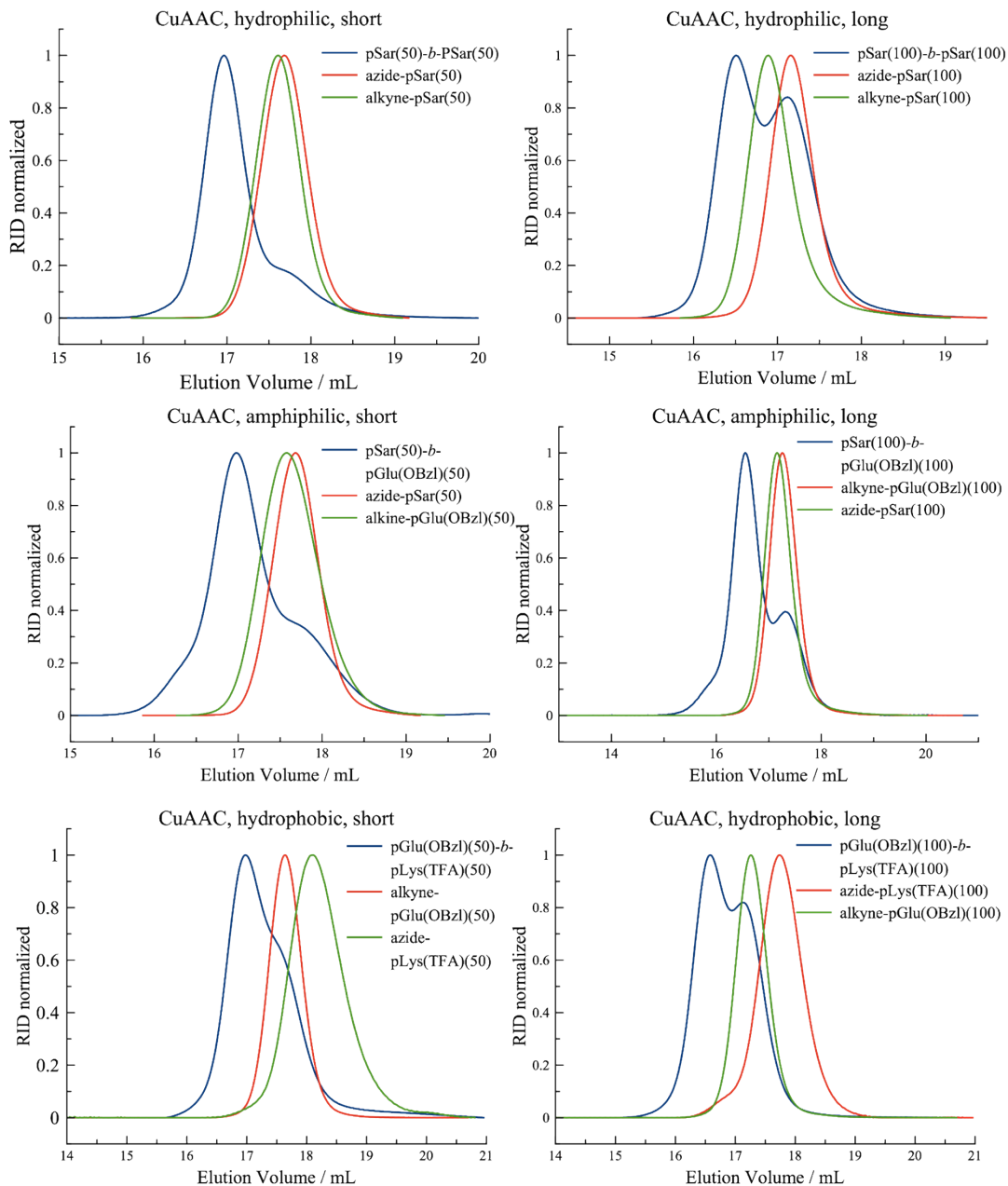


Figure 34: HFIP GPC elograms of ligation products and corresponding homopolymers for CuAAC.

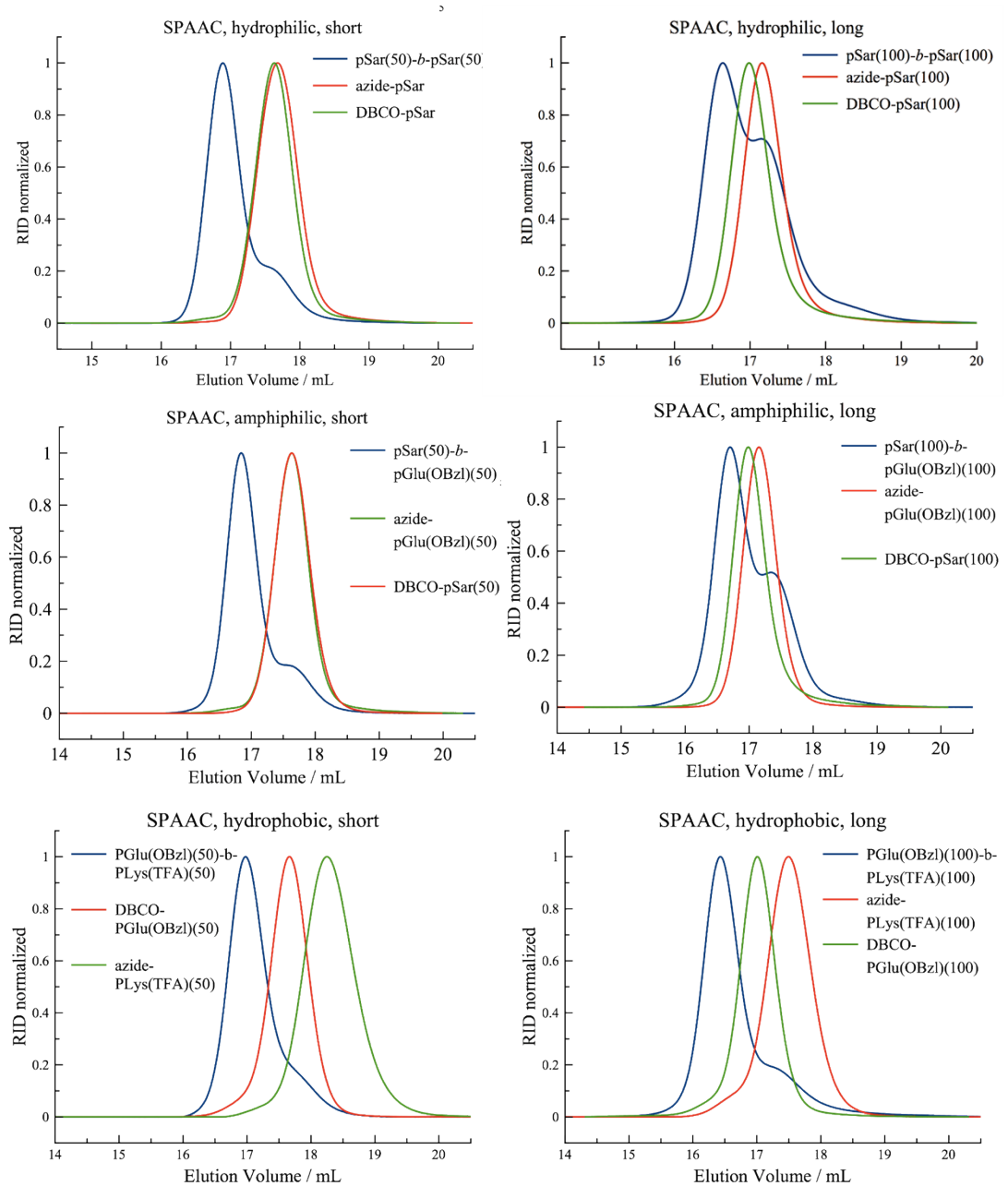
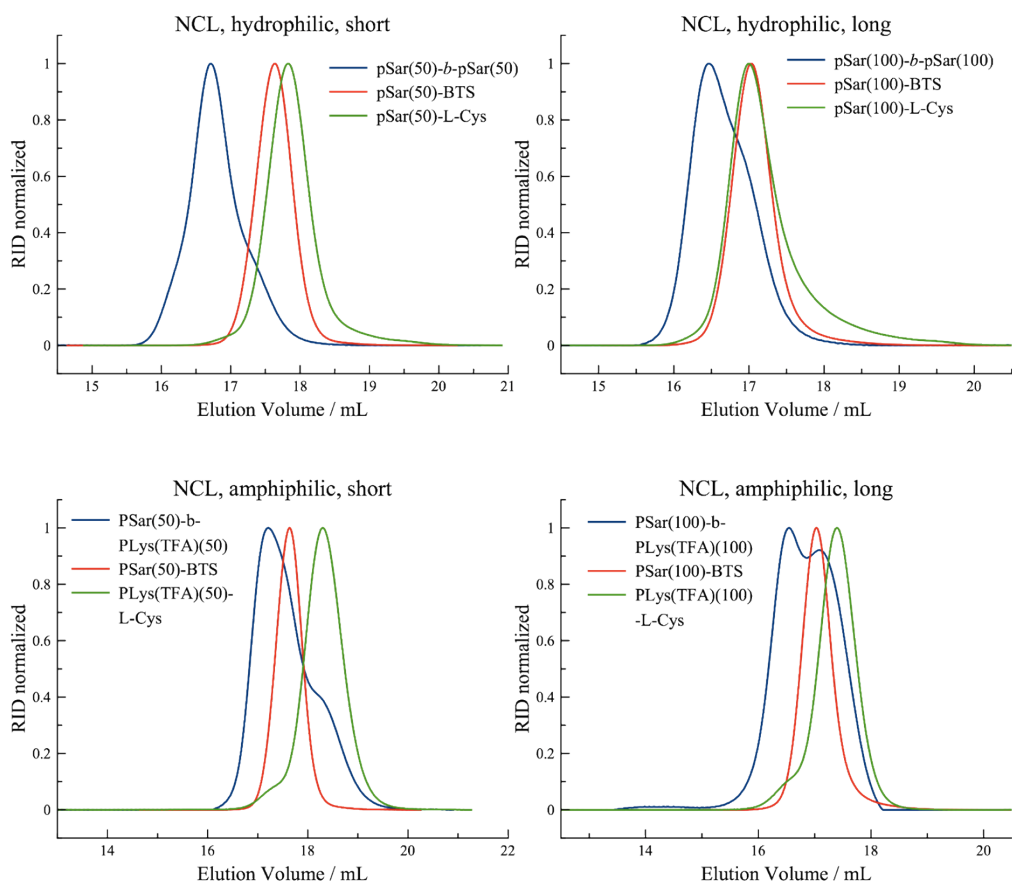


Figure 35: HFIP GPC elugrams of ligation products and corresponding homopolymers for SPAAC.



[Figure 36: HFIP GPC elugrams of ligation products and corresponding homopolymers for NCL.](#)

4. Fitting of GPC curves

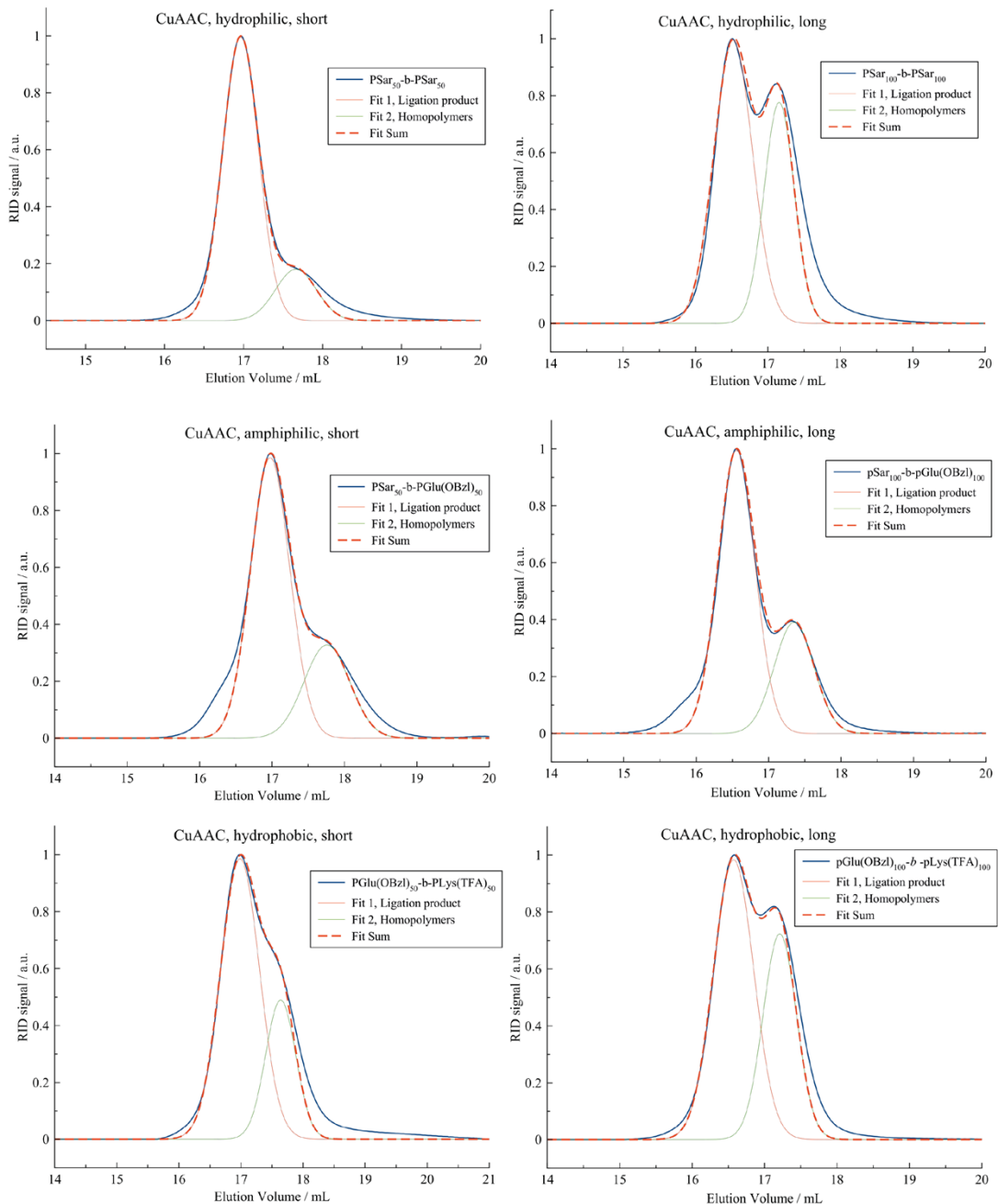


Figure 37: Gauss-fitted GPC curves of ligation products obtained by CuAAC.

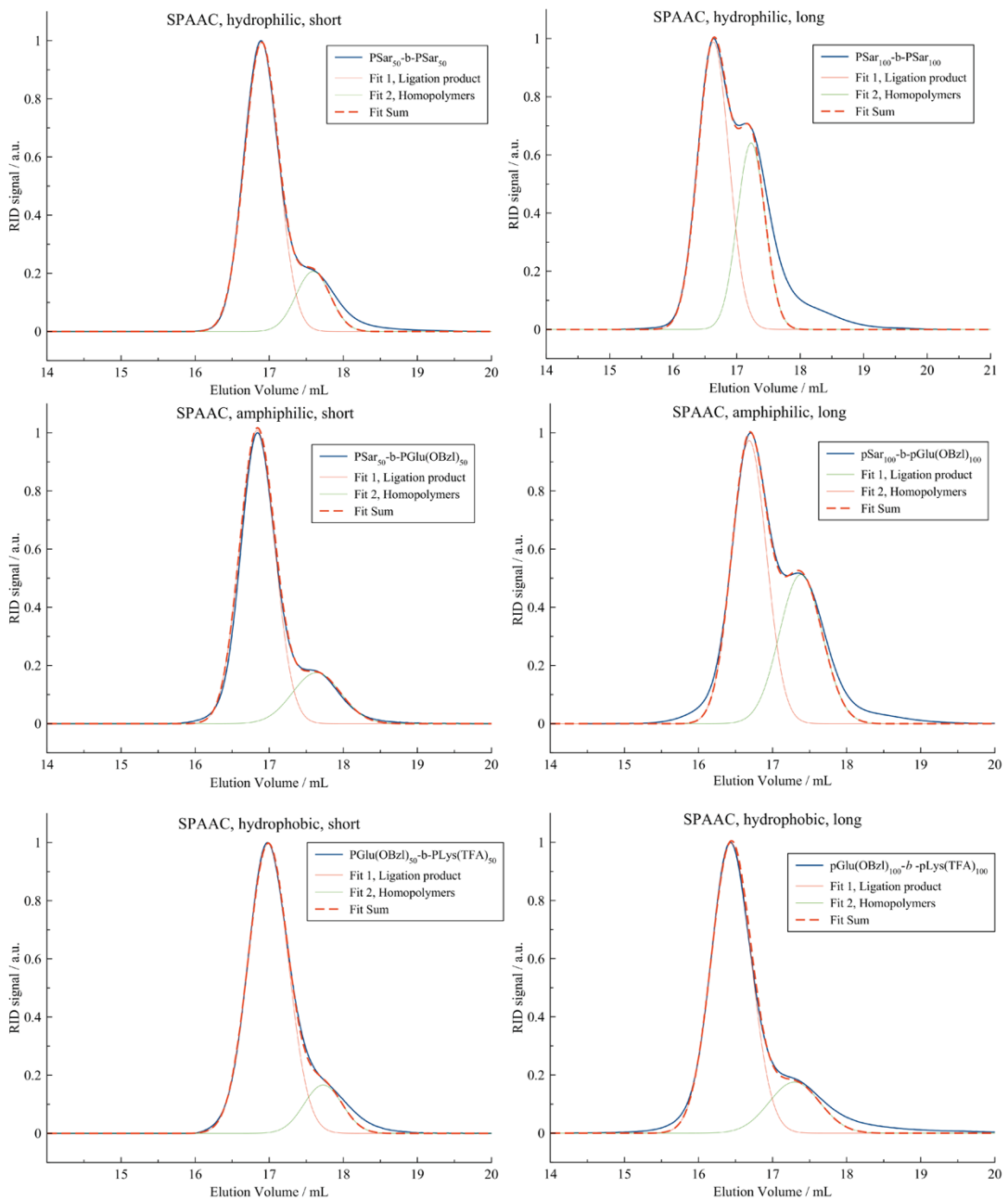


Figure 38: Gauss-fitted GPC curves of ligation products obtained by SPAAC.

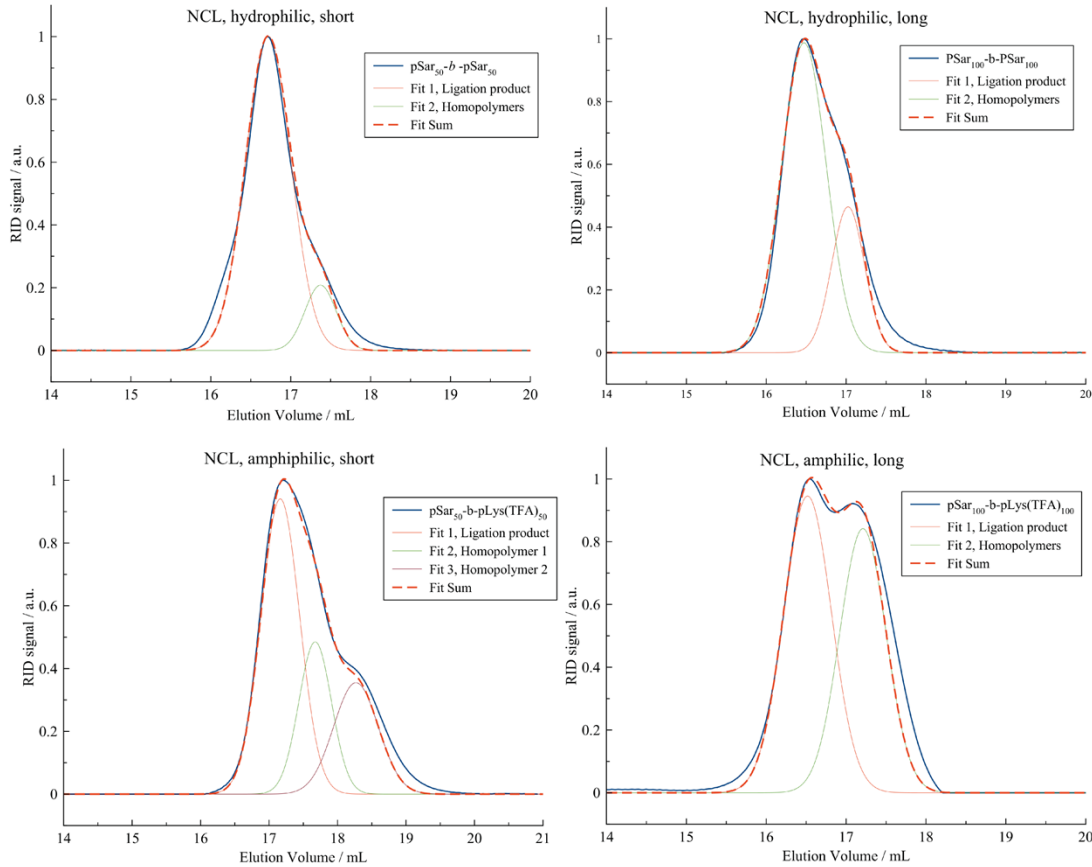


Figure 39: Gauss-fitted GPC curves of ligation products obtained by NCL.

Table 1: Determined efficiencies for conducted ligation experiments by Gauss fits.

Ligation	Polarity	Length	Determined Efficiency
CuAAC	hydrophilic	Short (50/50)	83
	hydrophilic	Long (100/100)	62
	amphiphilic	Short (50/50)	72
	amphiphilic	Long (100/100)	70
	hydrophobic	Short (50/50)	72
	hydrophobic	Long (100/100)	62
SPAAC	hydrophilic	Short (50/50)	83
	hydrophilic	Long (100/100)	63
	amphiphilic	Short (50/50)	81
	amphiphilic	Long (100/100)	66
	hydrophobic	Short (50/50)	86
	hydrophobic	Long (100/100)	82
NCL	hydrophilic	Short (50/50)	88
	hydrophilic	Long (100/100)	74
	amphiphilic	Short (50/50)	53
	amphiphilic	Long (100/100)	56

5. MTT Assay

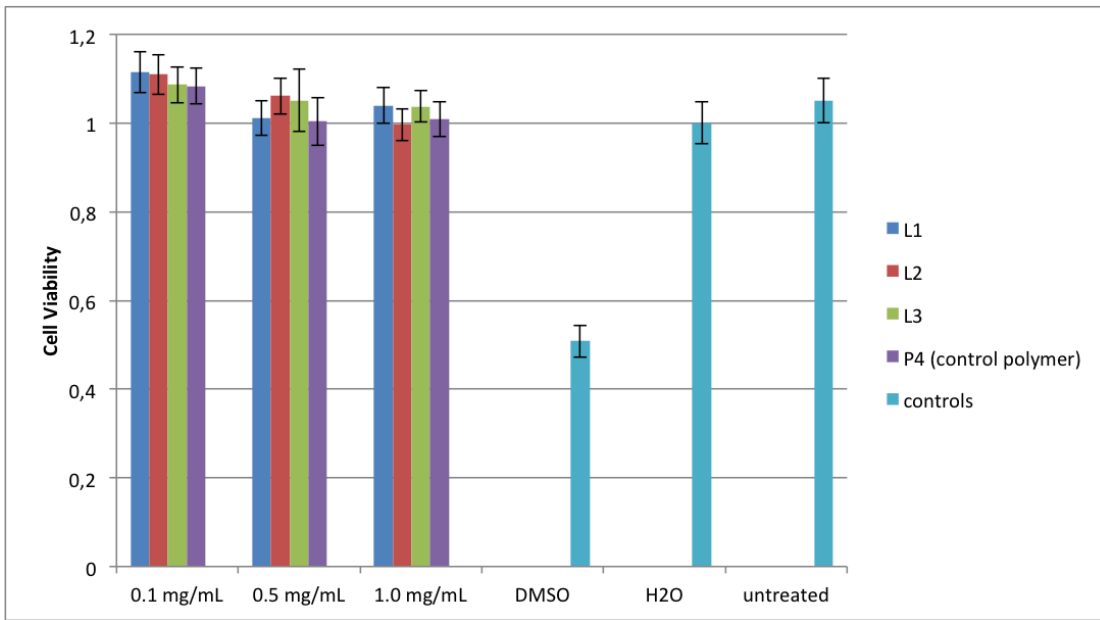


Figure 40: Evaluation of cytotoxicity for L1, L2, L3, P4 = PSar₁₀₀, DMSO, H₂O and untreated as controls.

6. MALDI-TOF MS

MALDI-TOF measurements were conducted on an AXIMA-CFR MALDI-TOF mass spectrometer. All mass spectra were recorded in the linear mode. The irradiation targets were prepared from trifluoroacetic acid solutions with 2,5-di-hydroxybenzoic acid as matrix and potassium trifluoroacetate as dopant. Samples with a concentration of 10 mg/mL in methanol were prepared and 10 µL of each sample were used per measurement. (4'-hydroxyazobenzene-2-carboxylic acid) (HABA) was employed as matrix material at a concentration of 10 mg/mL. 0.1 M NaTFA solution was added as dopant (1 µL).

MALDI-TOF MS was measured for P1 modified with S-benzylthiosuccinate (NPA+BTS) (PSar₆₀), P3 modified with protected cysteine (NPA+Boc-L-Cys(Trt)) (PSar₄₄-Boc-L-Cys(Trt)), P4 (PSar₄₄-APA), P6 (PSar₅₀-PA) and P8 (PSar₅₀-DBCO). Obtained data is summarized in table 2.

Table 2: Degree of polymerization (DP_n), dispersity and end groups determined by MALDI-TOF MS.

	Polymer	Initiator	DP _n	D	End group / g·mol ⁻¹	Expected End group / g·mol ⁻¹
P1 (BTS)	PSar	NPA	57	1.01	294.63	293.14
P3 (Cys)	PSar	NPA	44	1.02	534.69	532.28
P4	PSar	APA	43	1.03	101.13	100.07
P6	PSar	PA	49	1.02	57.25	55.04
P8	PSar	DBCO	45	1.02	277.91	276.13

7.1 MALDI-TOF Spectra

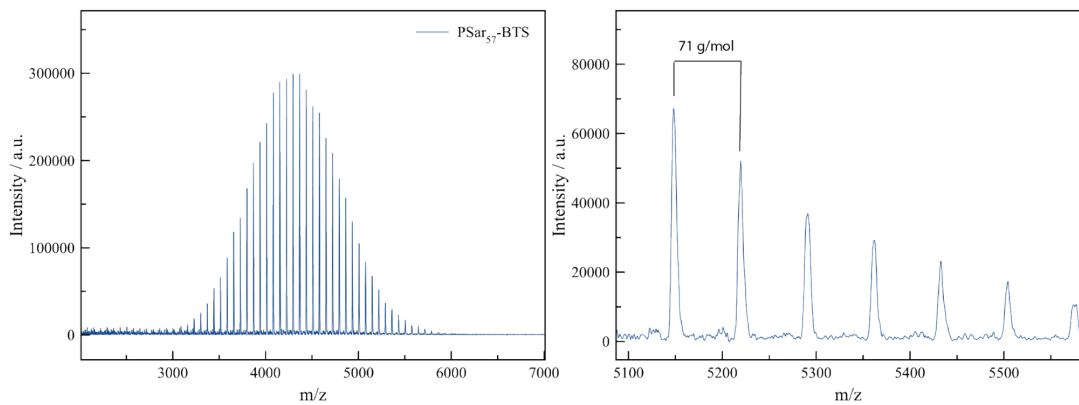


Figure 41: MALDI-TOF MS of PSar-BTS (RU = 71 g/mol); polymer + Na⁺.

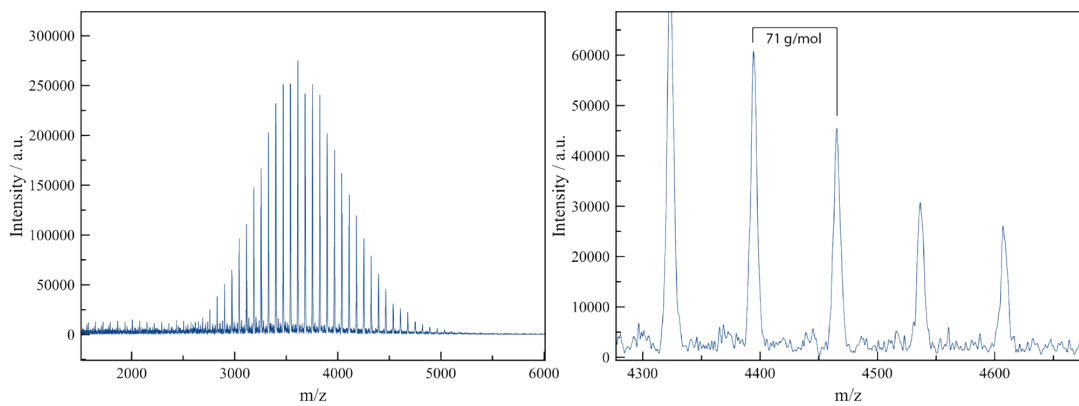


Figure 42: MALDI-TOF MS of PSar-Boc-L-Cys(Trt) (RU = 71 g/mol); polymer + Na⁺.

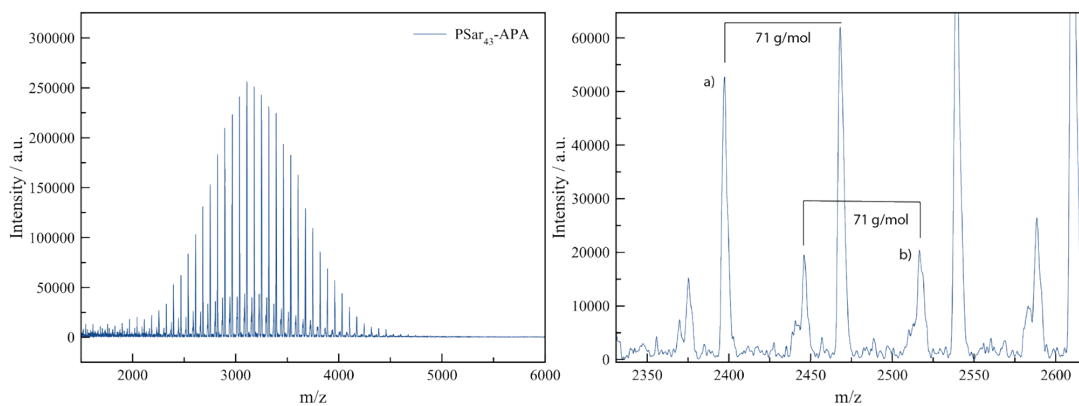


Figure 43: MALDI-TOF MS of PSar-APA (RU = 71 g/mol); a) polymer + Na⁺, b) polymer + H⁺.

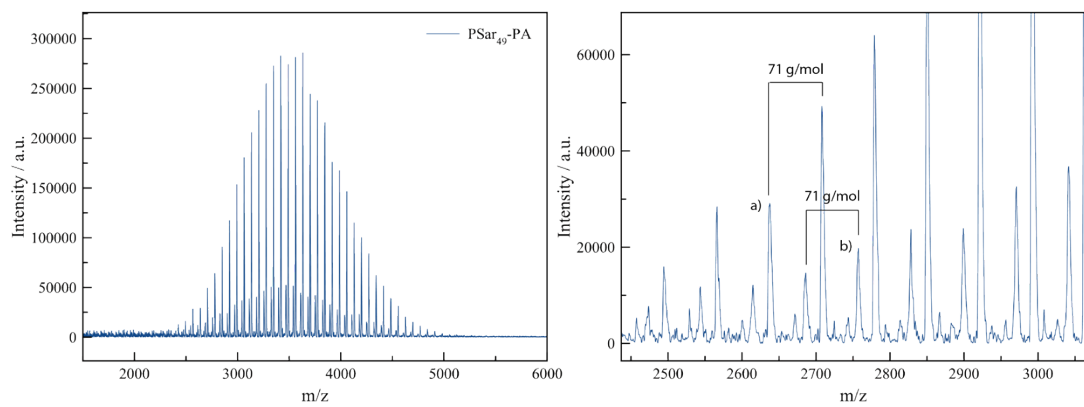


Figure 44: MALDI-TOF MS of PSar-PA (RU = 71 g/mol); a) polymer + Na^+ , b) polymer + H^+ .

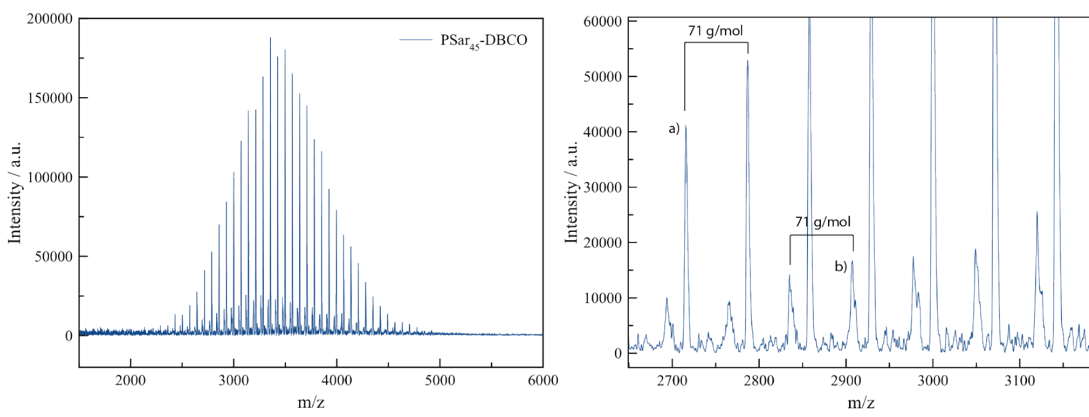


Figure 45: MALDI-TOF MS of PSar-DBCO (RU = 71 g/mol); a) polymer + Na^+ , b) polymer + H^+ .